SAPIENZA
UNIVERSITÀ DI ROMA

Dottorato di Ricerca in Neuroscienze del Comportamento XXXI Ciclo
Curricula di Neuropsicologia e Neuroscienze Cognitive

Neuroanatomy of The Bipolar Brain: From Brain Structure to Treatment

Candidate
Daniela Vecchio
Number 1050862

Coordinator
Prof. Stefano Ferraina

Tutor
Prof. Cecilia Guariglia

A.A. 2017-2018

To my family

INDEX

Acknowledgement

The studies here presented were developed at the IRCCS Santa Lucia Foundation, Neuropsychiatry Laboratory. I would like to address my gratification to Dr. Gianfranco Spalletta that allowed me to do this experience and to Dr. Fabrizio Piras and Dr. Federica Piras for their constant support. They helped me to overcome the various obstacles encountered in these years, in a priceless way, offering me a very fertile soil to grow. I also thank Dr. Valentina Ciullo, Dr. Nerissa Banaj, Dr. Tommaso Gili and all members of Neuropsychiatry Laboratory as their kindly presence had surrounded my daily work activities, making it really special as learning and working moments. As a work team, all of them contributed to make my PhD course period really stimulant and enriching, both from the professional and personal points of view. My gratifications also come to Neuroimaging Laboratory at the IRCCS Santa Lucia Foundation, to all persons and researcher working there, as they endured my constant presence and supported me in all my working needs.

A special thank is for both patients and healthy controls that I tested during this period, for their collaboration and availability to spend with me so much hours of their time.

Finally, the most special thanks are for my loved ones. My partner Luca, because he has never been tired of supporting my efforts and for my parents and my family because I always felt

close to them, even despite the kilometers that separated us because of my work.

About this work

Since the beginning of my PhD course, my efforts have been aimed to constantly improve my knowledge about neuroimaging techniques and methodologies. I further deepened a promising, challenging and intriguing way to *in vivo* investigate neuroanatomical cerebral correlates of behavioural diseases, applying these techniques to neuropsychiatric research. Neuroimaging studies are widely diffused in neuroscientific research, with the aim to improve diagnostic and prognostic processes, but also to better characterise patients' pharmacological and clinical aspects. However, despite the efforts made so far, unanimous consensus on the neuropathological substrates on many of the more disabling psychiatric conditions is still missing.

In this thesis, I summarised results from researches done during my PhD course, organising them in a brief introduction and five chapters. Specifically, the first chapter of this work is dedicated to the progress made during the past years in neuroimaging technologies and techniques, with a focus on structural Magnetic Resonance Imaging techniques and their employment into the neuropsychiatric research.

The following three chapters are dedicated to the three studies, all developed though a specific research topic and directed to the understanding of the neural basis of Bipolar Disorder and its clinical implications.

The first cross-sectional case-control study I presented in chapter two was aimed at understanding whether white matter and grey matter changes are present from the beginning of the illness and whether they continue to be present over the course of the disease, in a sample of 78 patients (BD) and 78 controls (HC). With respect to HC, the study found that patients with BD showed a reduced brain volume in areas comprising the posterior cingulate cortex bilaterally, the right thalamus, the bilateral cerebellum and the left posterior limb of the internal capsule. The fact that these areas were permanently reduced over the entire age range investigated, suggests that brain alterations are present from the very early phase of the disorder, and that they are not the results of a neurodegenerative process.

The second and the third studies I presented in chapters three and four are characterized by a strong clinical relevance, since they assessed the effect of lithium treatment (the gold standard treatment for BD patients) on brain structure. Specifically, study 2 was aimed at investigating the effects of lithium-treatment duration on the volumes of limbic and subcortical structures by comparing the groups of patients, stratified according to lithium exposure, (15 patients with a lithium exposure of less than 24 months (short-exposure group [SE]), and 15 patients naïve to treatment with lithium (no-exposure group [NE]) and HC. No differences in limbic and subcortical gray matter volumes were found between LE and HC. Hippocampal and amygdalar volumes were larger bilaterally in both LE and HC when compared to NE.

Amygdalar volumes were larger bilaterally in SE when compared to NE but did not differ from LE. Hippocampal volumes were smaller bilaterally in SE when compared to LE and HC but did not differ from NE. The study supports the idea that the effect of lithium exposure on limbic and subcortical gray matter volumes appears to be time-dependent and relatively specific to the hippocampus and the amygdala, with short-term effects on the amygdala and long-term effects on both structures.

For the third study, I employed a recent structural neuroimaging approach (i.e. shape analysis) which allows the quantification of advanced morphometric features of deep grey matter structures. In this study, I tested the hypothesis that shape characteristics of deep grey matter structures in bipolar disorder are associated with the duration of lithium treatment, finally impacting clinical phenomenology. The sample was composed of BD naïve to lithium treatment (NoLi), BD with short-term lithium treatment (LiTD-), BD with long-term lithium treatment (LiTD+), and HC. Results revealed a significant bilateral extroflexction effect dependent to increased duration of lithium treatment on the core of BD accumbens surfaces, while a concomitant introflection effect was found on the shell of right accumbens. A further analysis between groups with different treatment duration, showed that NoLi e LiTD- groups had inward/outward deformations both on left core and on the right shell of the accumbens surfaces when compared to HC and LiTD+. Moreover, the deformation of L-Accu-Core

shape was significantly correlated with increased depression severity.

Finally, a conclusive chapter summarizes results and implications of the presented works.

Introduction

The desire to understand the human mind has been one of the main desires of philosophers throughout the ages. During the last century, questions about cognitive and emotional process as well as about their cerebral neuroanatomical correlates have lead physician, psychologists, computer scientists, physicist to converge in the current discipline that is cognitive neuroscience.

Non-invasive imaging of the human brain has proven invaluable in this context. Indeed, neuroimaging technologies have enabled the investigation of normal brain functions and are being used to gain important new insights into the mechanisms behind many neuropsychiatric disorders. This research has implications in identifying biomarkers of disease, prognosis, treatment effects, elucidate biological pathways, and help redefine diagnostic boundaries and inform and monitor new therapies.

Unlike many neurological diseases, psychiatric disorders do not cause changes that are visible to the naked eye in the neuroimaging study of the individual patient (Agarwal et al., 2010). They are, however, amenable to investigation by recent neuroimaging modalities, particularly quantitative structural imaging. This was the reason for the rapid growth of magnetic resonance imaging

(MRI) research of psychiatric disorders. It has reflected the aspirations of many psychiatrists and neuropsychologist to link the signs and symptoms of psychiatric disease to specific brain structural abnormalities.

Bipolar disorder (BD) is an especially good example of a group of psychiatric illnesses that are difficult to diagnose accurately. Specifically, BD is a mental health condition defined by periods (better known as episodes) of extreme affective disturbances, marked by alternating status of mood elation (mania/hypomania) and depression interspersed by euthymic (normal mood) periods. There are two main types of bipolar disorders: bipolar type I and bipolar type II. According to the DSM 5 (American Psychiatric Association. DSM-5 Task Force., 2013), BD type I involves episodes of severe mania and often depression, while BD type II involves a less severe form of mania called hypomania and depressive episodes are more frequent than in type I.

Although BD, along with other psychiatric illnesses, is one of the ten most debilitating of all non-communicable diseases (Department of Health Statistics and Informatics, 2008), misdiagnosis of the illness as recurrent unipolar depression occurs in 60% of patients seeking treatment for depression (Goodwin and Jamison, 2012; Hirschfeld et al., 2003). Structural neuroimaging data had provided evidence for the assumption that Bipolar disorder are not exclusively functional illnesses but also show a diversity of

morphological changes. They allow investigation on potential neurodevelopmental and neurodegenerative processes involved in the disease and in their specific time course. Indeed, the identification of objective neuroimaging biomarkers that represent pathophysiologic processes that differ between bipolar disorder and other psychiatric diseases can both inform bipolar disorder diagnosis and provide biological targets for the development of new and personalized treatments. This is mostly important at the presentation of first episodes of the disorder, when different diagnosis can show confounding symptomatology overlapping (Rosen *et al.*, 2012).

As the size of the experimental cohorts grew, studies began to examine brain patterns associated with heterogeneous expression of clinical symptoms, the mechanisms of disease progression, and even differential patterns of treatment response.

CHAPTER 1

NEUROIMAGING

1.1 History of Neuroimaging

In the last twenty years, neuroimaging of the brain has advanced at a tremendous pace because of technological innovations, developments in computing and new statistics that have been developed to interrogate neuroimaging data.

The history of modern *in vivo* imaging began from the side of the structural tissue visualization, with radiographic techniques. However, since the brain is composed of soft tissue, that is not radio-opaque, it remained essentially invisible to plain X-ray investigations. The first attempt to visualize the brain traces back to 1918, when the work of the neurosurgeon Walter Dandy (Kilgore and Elster, 1995) on experimental hydrocephalus and cerebrospinal fluid circulation led to the development of pneumoencephalography (Sampath *et al.*, 2000). Most of cerebrospinal fluid was temporarily replaced trough a lumbar puncture with a contrast agent such as air, oxygen or helium, to improve brain contrast when imaging it with X-rays. It was derived from ventriculography, an earlier method where the air was injected through holes drilled in

the skull of the patient. Pneumoencephalography become a common medical procedure mostly used to evaluate the size of brain ventricles until the late 1970s. In 1927, Egas Moniz, neurologist and winner of the Nobel Prize in Physiology or Medicine (1949) for the discovery of leucotomy (Fusar-Poli *et al.*, 2008), introduced cerebral angiography, which allowed visualizing with great accuracy blood vessels in and around the brain (Ligon, 2003). Drawbacks of these early methods were that the signal-to-noise ratio was poor, and that, being invasive techniques, the risk and discomfort for the patients were significantly high.

Non-invasive structural brain imaging method was computerized tomography (CT), developed in the late 1970s, when minicomputers and transverse axial scanning method became available. Transverse axial scanning was largely due to the work of Godfrey Hounsfield and Allan McLeod Cormack (Raju, 1999), who won the 1979 Nobel Prize for Physiology or Medicine for their work (Montgomery, 1979). With the CT available, better quality anatomical images of the brain became accessible to both clinicians and researchers. About a decade later, in the early 1980s, a second non-invasive structural brain imaging method, Magnetic Resonance Imaging (MRI), was introduced clinically. It was developed thanks to the work of several researchers who buit its theoretical bases [for a detailed review, see (Geva, 2006)], including Peter

Mansfield and Paul Lauterbur. These researchers independently published in 1974 the technique that later became known as MRI (initially named Nuclear Magnetic Imaging – NMI), and were awarded the Nobel Prize for Physiology or Medicine in 2003 (Pincock, 2003). With regard to patient safety, MRI was superior to CT scan because CT scan is using ionizing radiation, while MRI uses harmless radio waves. Consequently, it has become the gold standard method to visualize non-invasively human brain structure, with a veritable explosion of technical refinements and diagnostic MR applications.

Specifically, a number of processes have been introduced and developed to produce MR images. These processes include nuclear alignment, orthogonal Radio Frequency (RF) excitation, spatial encoding, and image formation. In simple terms, an MRI system consists of five major components: a) a magnet (to produce the B_0 magnetic field for aligns protons), b) gradient systems (to spatially encode the positions of protons into the x/y/z axes), c) an RF coil system (to excite protons and perturb their alignment), d) a receiver (to register radio signals), and e) a computer system (to control the whole system and reconstruct the images). MRI development was based on knowledge that the human body is mostly made of water. Water molecules (H_2O) contain hydrogen nuclei (protons), which become aligned in a magnetic field. An MRI scanner applies a very strong magnetic field (about 0.2 to 7 teslas, or

roughly a thousand times the strength of a typical fridge magnet), which aligns the proton "spins." The scanner also produces a radio frequency current that creates a varying magnetic field. The protons absorb the energy from the magnetic field and flip their spins. When the field is turned off, the protons gradually return to their normal spin, a process called precession. The return process produces a radio signal that can be measured by receivers in the scanner and made into an image. Protons in different body tissues return to their normal spins at different rates, so the scanner can distinguish among various types of tissue. The scanner settings can be adjusted to produce contrasts between different body tissues. Additional magnetic fields are used to produce 3D images, that may be viewed from different angles (Rodriguez, 2004).

The enhancement of these non-invasive neuroimaging techniques (together to other subsequently developed imaging tools, like positron emission tomography - PET, electroencephalography - EEG, and magnetoencephalography - MEG), have enabled the *in vivo* visualization and analysis of the brain function and structure in unprecedented detailed manner. Moreover, they transformed the way we study the nervous system under normal and pathological conditions (Kikinis *et al.*, 2014), particularly in neuropsychiatric disorders (Mayberg, 2014).

1.2 Neuroimaging Modalities and Technical Aspect

Traditionally, the brain imaging modality has been divided into structural (Symms *et al.*, 2004) and functional neuroimaging (Raichle, 2009); even if, more novel neuroimaging modalities provide an admixture of the two and do not fit pristinely into this dichotomy (e.g. Diffusion Tensor Imaging - DTI) (Jones and Leemans, 2011).

Functional neuroimaging is the use of neuroimaging technology to measure an aspect of brain function, often with the aim to understanding the relationship between activity in certain brain areas and specific cognitive functions (Raichle, 2009). Common methods of functional neuroimaging include Positron Emission Tomography (PET), Functional Magnetic Resonance imaging (fMRI), Electroencephalography (EEG), Magnetoencephalography (MEG), Functional Near-Infrared Spectroscopy (fNIRS), Single-Photon Emission Computed Tomography (SPECT) (*ibidem*).

From the other side, structural neuroimaging provides a powerful tool to map the anatomy of the brain (Symms *et al.*, 2004). Presently, there are essentially two structural neuroimaging modalities that are commonly used in clinical settings and in neuroscientific research, CT and structural MRI (sMRI). Both techniques yield images with excellent spatial resolution and contrast and are widely used to assess cerebral pathology in neuropsychiatric disorders. From the

perspective of practicing psychiatrists both techniques are important and they are now readily available and increasingly affordable.

I focus on human brain imaging with MRI recognizing that other techniques (e.g. PET, SPECT and CT), particularly electrical (e.g. EEG, MEG and ECoG), also have and will continue to have an important role in neuroscience.

1.2.1 Functional Magnetic Resonance Imaging

Functional MRI (fMRI) makes use of the same hardware as MRI but exploits the paramagnetic properties of cerebral blood flow (CBF) (Villringer and Dirnagl, 1995). The commonest method of fMRI relies on the variations in signal intensity that occur as a consequence of altered levels of cerebral blood oxygenation. This technique is called Blood Oxygen Level-Dependent (BOLD) contrast and is currently the mainstay of human neuroimaging, since its discover (Ogawa *et al.*, 1990). It is based on the assumption that regional neural activity results in increased local CBF, producing an increase in oxyhaemoglobin and carrying red blood cells. This essentially leads to a net decrease in de-oxyhaemoglobin. The two molecules oxyhaemoglobin and de-oxyhaemoglobin have different magnetic properties (diamagnetic and paramagnetic

respectively) and the relative change in concentrations of the two results in a change in signal intensity (*ibidem*).

Typically, fMRI is used to identify brain regions that are activated by a specific task performed by an individual whilst in the scanner (Campanella *et al.*, 2017; D'Esposito *et al.*, 1998). It is important to note, however, that it does not detect actual neuronal transmission but instead relies on the presumed coupling of neural responses to local blood flow. It is therefore used to assess neuro-cognitive processes, and the concurrent acquisition of structural MRI allows the regions of activity to be accurately mapped onto images of the brain. The advantages of fMRI over other techniques is that it is non-invasive and allows the study of brain function without the use of ionising radiation or the injection of radiopharmaceuticals that are used by other (like PET and SPECT). In practice, fMRI can be conducted on most clinical 1.5 Tesla MR scanners, using conventional hardware, although some additional software is often needed. Nowadays, high field scanners (3 Tesla) are more common and are the preferred choice as they afford greater signal-to-noise ratio. In comparison to other modalities fMRI offers the best spatial resolution, however, it is susceptible to a number of artefacts, the most limiting of which is caused by movement. Hence, in most fMRI experiments it is necessary for subjects to lie extremely still for up to 40 min and this makes it difficult to apply to some

psychiatric disorders such as panic disorder and mania (Wylie *et al.*, 2014).

1.2.2 Structural Magnetic Resonance Imaging

As mentioned before, MRI takes advantage of the fact that certain atoms when placed in a magnetic field align with the direction of the field. In an MRI scanner, this pattern of alignment is predictably disrupted by radio-frequency (RF) waves that are turned on and off systematically to yield pulses of energy that are then measured and processed into images. Hydrogen is the most commonly imaged element in MRI because of its abundance and because it gives the strongest signal. The nucleus of a hydrogen atom is a single spinning proton with a positive charge that generates a tiny magnetic field. Normally, the field surrounding hydrogen atoms is orientated randomly and together the fields of many hydrogen atoms cancel out. However, when in a large external magnetic field (B0) such as that of the MRI scanner the protons align with the direction of the field and *precess* about B0 at a frequency called the Larmor frequency, and lie in the RF range. If then an RF pulse of this frequency is directed into the tissue the spinning protons resonate and precess in phase. This generates a transverse magnetic field that precesses at the same Larmor frequency. When the RF pulse is switched off

the precessing protons induce an electromagnetic field in a detector coil outside the tissue that can be measured and subsequently powerful computers process this raw data to produce the MRI images (Rodriguez, 2004).

Based on MRI principles, sMRI technique translates the local differences in water content into different shades of gray, that serve to outline different brain regions shape and size. The two main characteristics which govern image quality are spatial resolution and signal to noise ratio (SNR). In-plane resolution is chiefly determined by the number of picture 3D elements (voxel) in the frequency and phase encoding directions, and through-plane resolution by the slice thickness. SNR is determined by voxel size, slice thickness, scan time (including the number of phase encoding steps) and the sequence used. Image quality is *therefore* ultimately determined by scan time, which, in turn, is influenced chiefly by patients' ability to comply with keeping still.

During the last three decades, structural MRI had emerged as an essential tool for morphometric techniques (including volumetric, shape analysis, and microstructural techniques) (Spalletta et al., 2018). These techniques helped clarify in vivo some of the principal neurobiological characteristic of major psychiatric (Chiapponi et al., 2018; Dusi et al., 2018; Janiri et al., 2018), neurological and neurodegenerative diseases (Lipp et al., 2018; De Marco and Venneri, 2018; Di Paola and Bourisly, 2018; Péran et

al., 2018; Schrader et al., 2018), but also of normal population studies (Matsuda, 2018; Tamnes and Østby, 2018) and cognitive neuroscience, in general (Morita *et al.*, 2016).

sMRI: sequences and terminology

The appearance of the brain on an image from an MRI scan is dependent on a number of interrelated factors (see Table 1). These include innate tissue properties that are described using parameters such a relaxation time and proton density, and are referred to as T1 and T2. Imaging techniques and protocols also determine the exact nature of the image obtained and terms that are frequently used in this context include sequences such as spin-echo, fast spin-echo, gradient-echo and echo-planar imaging with varying echo times (TE), flip angles and repetition times (TR). A T1-weighted image has a short TR and short TE such that tissues with a short T1 relaxation time appear bright and those with a long T1 appear dark. On a T2-weighted image that has long TR and long TE, tissues with a short T2 relaxation time are dark and those with a long T2 are bright (Rodriguez, 2004).

Images from conventional T1-weighted (T1-w) and T2-weighted (T2-w) MRI sequences, are characterized by a high contrast and spatial resolution, being widely used to

investigate structural properties of the brain (Ganzetti *et al.*, 2015), used for volumetric study (Spalletta *et al.*, 2018). Pathological processes are therefore most often described in terms of T1 and T2 signal behavior that results in a computer-generated image with a highly detailed map of the brain's tissues and structures. Thus, this tool can be used to discover the presence of abnormal tissue through the changes in tissue density or composition. Scientists, clinician and neuroradiologist examining an sMRI can readily distinguish between gray and white matter and other types of tissue—both normal, such as blood vessels, and abnormal, such as tumors—by their different shading and contrast with surrounding areas.

Table 1

	Appearance on MRI image		
Scanned Tissue	T1-Weighted	T2-Weighted	Flair
CSF	Dark	Bright	Dark
White Matter	Light	Dark Gray	Dark Gray
Cortex	Gray	Light Gray	Light Gray
Fat	Bright	Light	Light
Inflammation (infection, demyelination)	Dark	Bright	Bright

CSF: cerebral-spinal fluid;

A third commonly used sequence is the Fluid Attenuated Inversion Recovery (FLAIR). FLAIR images are heavily similar to T2-weighted images, except that the

TE and TR times are very long. By doing so, abnormalities remain bright but normal CSF fluid is attenuated and made dark. It has been introduced as a complement of, or even a replacement for, the conventional T2-weighted sequence. Indeed, setting to null fluids using an inversion time that effectively suppresses hyperintense signals from free water in cerebrospinal fluid (CSF), FLAIR sequences allow to highlight hyperintense coming from tissues' lesions (De Coene *et al.*, 1992). Hence, this sequence is very sensitive to pathology and makes the differentiation between CSF and an abnormality much easier (Fukuoka *et al.*, 2010; Iorio *et al.*, 2013; Sati *et al.*, 2012).

1.2.4 Diffusion Neuroimaging

A more recent brain imaging technique, which has emerged from advances in MRI, is that of Diffusion Weighted Imaging (Bammer, 2003) and Diffusion Tensor Imaging (Mori and Zhang, 2006) (respectively, DWI and DTI). These last takes advantage from specific MRI sequences as well as software that uses the diffusion of water molecules to generate contrast in MR images.

Diffusion weighted imaging is an MRI modality that enables the quantification of the diffusion of water in tissue making it possible to investigate microstructural aspect of the white matter, within the brain. It is predicated on the fact

that anatomical structures such as cell membranes, myelin sheaths, as well as intracellular micro-organelles act as barriers to the diffusion and free movement of water thus limiting the spatial flow of these molecules. The arrangement of axons in parallel bundles with myelin sheaths facilitates the diffusion of water molecules longitudinally, preferentially along their main direction. Such preferentially oriented diffusion is called anisotropic diffusion (Mori and Zhang, 2006). By acquiring a conventional diffusion weighted MRI in at least six non-collinear directions it is possible to reconstruct the brain's underlying neuronal microstructure that is normally 'invisible' using conventional MRI (Schilling *et al.*, 2017).

A special kind of DWI, DTI, has been used extensively to investigate and to map white matter microstructural integrity and tractography in the brain (Davis *et al.*, 2009; Lazar *et al.*, 2003; Melhem *et al.*, 2002). Tractographic reconstruction of neural connections via DTI is based on an extension of diffusion MRI properties. Indeed, if a series of diffusion gradients (i.e. magnetic field variations in the MRI magnet) are applied in a fashion that can determine at least 3 directional vectors (use of 6 different gradients is the minimum and additional gradients improve the accuracy for "off-diagonal" information), it is possible to calculate, for each voxel, a tensor (i.e. a symmetric positive definite 3×3 matrix) that describes the 3-dimensional shape of diffusion (Mori and

Zhang, 2006; Mori and van Zijl, 2002; Schilling *et al.*, 2017). Specifically, the fiber direction is indicated by the tensor's main eigenvector. This vector can be color-coded, yielding a cartography of the tracts' position and direction (red for left-right, blue for superior-inferior, and green for anterior-posterior) (Alexander *et al.*, 2007; Jones and Leemans, 2011). Characterization of each eigenvalue (λ) in the tensor and combinations (see. Table 2) of them help constitute the main diffusion measures, offering information of microstructural aspects. In DTI studies, there are four measures that are most commonly used; fractional anisotropy (FA), mean diffusivity (MD), axial diffusivity (AD) and radial diffusivity (RD). Specifically, in axial diffusivity (AD) we only quantify the value of λ1. While in radial diffusivity (RD) we take the average of λ2 and λ3. Mean diffusivity (MD) provides an average of all. And finally, fractional anisotropy (FA) provides the relative difference between the largest eigenvalue as compared to the others. These measures are commonly used clinically to localize white matter lesions that do not show up on other forms of clinical MRI (Alexander *et al.*, 2007).

Table 2

	FA	MD $(\lambda1+\lambda2+\lambda3)/3$	AD $\lambda1$	RD $(\lambda2+\lambda3)/2$
	FA is a summary measure of microstructural integrity. While FA is highly sensitive to microstructural changes, it is less specific to the type of change.	MD is an inverse measure of the membrane density, is very similar for both GM and WM and higher for CSF. MD is sensitive to cellularity, edema, and necrosis.	AD tends to be variable in WM changes and pathology. In axonal injury AD decreases. The ADs of WM tracts have been reported to increase with brain maturation.	RD increases in WM with de- or dys-myelination. Changes in the axonal diameters or density may also influence RD.
Gray Matter	↓	–	↓	↑
White Matter	↑	–	↑	↓
CSF	↓	↑	↑	↑
High myelination	↑	↓	–	↓
Dense axonal packing	↑	↓	–	↓
WM Maturation	↑	↓	↑	↓
Axonal degeneration	↓	↑	↓	↑
Demyelination	↓	↑	–	↑
Low SNR	↓	↑	↓	–

CSF: cerebrospinal fluid; WM: white matter; SNR: signal-to-noise ratio; FA: Fractional Anisotropy; MD: Mean Diffusivity; AD: Axial Diffusivity; RD: Radial Diffusivity; λ: eigenvalue

A further advance of DTI is its application to non-invasively construct 3D trajectories of neural tracts in-vivo, using tractographic techniques (Lazar *et al.*, 2003). Specifically, fiber tracking algorithms can be used to track a fiber along its whole length (e.g. the corticospinal tract, through which the motor information transit from the motor cortex to the spinal cord and the peripheral nerves). Tractography is a useful tool for measuring deficits in white

matter, such as in aging (Davis *et al.*, 2009). Its estimation of fiber orientation and strength is increasingly accurate, and it has widespread potential implications in the fields of cognitive neuroscience and neurobiology. Tractography also allows the modelling of white matter neural connectivity, a method that is currently the subject of intense investigation as it can provide information relating to neuronal connections (Rubinov and Sporns, 2010). At this point in time the ability of DTI to characterize the white matter architecture of the brain is unparalleled by any other imaging modality.

2. Structural Neuroimaging in Psychiatric Disorders

Advances in neuroscience have revolutionized our understanding of the central nervous system leading to new insights into the complex anatomical, physiological, biochemical, genetic, and molecular organizational structure of the human brain. Specifically, neuroimaging technologies have enabled the investigation of normal brain function/structure and are being used to gain important new insights into the mechanisms behind many neuropsychiatric disorders. Indeed, since the demonstration, in 1976, that patient with schizophrenia had enlarged cerebral ventricles (Johnstone *et al.*, 1976), psychiatry was pushed in a new era where neuroimaging would help it identify mental disorders

and ultimately clarify their mechanisms. Thanks to structural brain neuroimaging, it is now widely accepted that schizophrenia is a neurodevelopmental disorder with neurobiological evidence (Chiapponi *et al.*, 2018). The fact that structural changes occur and are discernible with neuroimaging methodologies has assisted in unravelling the pathophysiology of schizophrenia, and of other major psychiatric condition, like mood disorders (Janiri *et al.*, 2018).

The research applications of neuroimaging in psychiatry, however, have to compound to several issues, intrinsically related to psychiatric illness. Indeed, they are usually primarily diagnosed by careful assessment of behavior combined with subjective reports of abnormal experiences to group patients into disease categories, that mask substantial heterogeneity. For example, a diagnosis of schizoaffective disorder is often given to people with episodes of both affective and psychotic symptoms, (either alternating or occurring together) which casts some doubt on the traditional dichotomy delineating affective and psychotic disorders into discrete illness categories (Craddock and Owen, 2005). In the absence of definitive and objective biomarkers of pathophysiological processes underlying behaviors associated with conventionally defined psychiatric illness categories, and because of the heterogeneity within, and considerable overlap between,

these behaviors, appropriate diagnosis and treatment are difficult for many psychiatric illnesses.

Bipolar disorder is an especially good example of a group of psychiatric illnesses that are difficult to diagnose accurately. For example, although this disorder, along with other psychiatric illnesses, is one of the ten most debilitating of all non-communicable diseases (Department of Health Statistics and Informatics, 2008), misdiagnosis of the illness as recurrent unipolar depression occurs in 60% of patients seeking treatment for depression (Goodwin and Jamison, 2012; Hirschfeld *et al.*, 2003). Moreover, bipolar disorder types I and II are especially difficult to diagnose accurately in clinical practice, particularly in their early stages. Only 20% of patients with bipolar disorder who are experiencing a depressive episode are diagnosed with the disorder within the first year of seeking treatment (Hirschfeld *et al.*, 2003), and the mean delay between illness onset and diagnosis is 5–10 years (Baldessarini *et al.*, 2007). A major reason for the difficult diagnosis is the challenge of differentiating bipolar disorder type I or II from unipolar depression — an illness characterized by recurrent depressive episodes — especially in patients who present during a depressive episode and in those with no clear history of mania or hypomania (Goodwin and Jamison, 2012; Hirschfeld *et al.*, 2003). This is further compounded by comorbid anxiety (Simon *et al.*, 2004), substance misuse (Cassidy *et al.*, 2001).

Neuroimaging technologies being used to gain important new insights into the mechanisms behind bipolar disorders. Limbic and cortical areas and circuits that are implicated in the generation and regulation of emotion have been the main focus in neuroimaging research, since they can be readily visualized and investigated using structural techniques. Hence, mood disorders, in general, and bipolar disorder neuroimaging research in particular, is now a substantive and promising field. The research applications of neuroimaging in bipolar disorder aim to relate psychopathology to structural and functional aspects of the brain and can be broadly viewed as having either a restructuring or refining role. *Restructuring* involves dispensing with the current psychiatric phenomenological entities and replacing these with biologically driven explanations based on neuroscientific findings. In contrast, *refining* involves generally maintaining the current categories of psychiatric disorders but validating their essential elements by providing a neural substratum. Both approaches find support in the many studies that have been conducted in bipolar patients populations.

3.1 Structural Neuroimaging in Bipolar Disorder

In DSM-5, bipolar and related disorders, as they are now called, are given a chapter on their own, that includes

bipolar I disorder, bipolar II disorder and cyclothymic disorder (American Psychiatric Association. DSM-5 Task Force., 2013). While in the past only a distinct period of abnormally and persistently elevated, expansive or irritable mood was necessary, these symptoms now have to be present in combination with persistently increased (goal-directed) activity or energy, most of the day, nearly every day.

Bipolar Disorder (BD) is a mood disorder that confers considerable individual and societal morbidity and cost (Gardner et al., 2006). Patients with BD experience recurrent episodes of marked mood changes, which last for at least a week, and may continue for months. These episodes consist of periods of mania or hypomania, depression, or mixed mood, interspersed with periods of normal mood (euthymia) (Belmaker, 2004). A significant body of evidence suggests that BD has a strong neurobiological basis and structural brain abnormalities in BD have been reported (Hallahan et al., 2011; Hibar et al., 2016), even if the pattern of these brain abnormalities based on magnetic resonance imaging is still not clearly defined.

White Matter

White matter (WM) abnormalities are one of the most consistently reported findings in neuroimaging studies of

BD (Vederine *et al.*, 2011). Indeed, the presence of white matter hyperintensities (WMH) on T2-weighted and FLAIR MRI scans was confirmed in several neuroimaging studies (Altshuler *et al.*, 1995; Gulseren *et al.*, 2006). Although the pathogenesis of WMH is not completely understood, at least some are likely to reflect vascular ischemia and are associated with cardiac risk factors and normal ageing (Matsusue *et al.*, 2006). Despite the association with age, a number of studies have reported WMH in young patients with bipolar disorder (Altshuler *et al.*, 1995; Breeze *et al.*, 2003; Lyoo *et al.*, 2002; Silverstone *et al.*, 2003). They appear particularly significant in affective disorder, having been associated high rates of suicidality (Pompili *et al.*, 2007).

DTI studies are a more recent promising approach for the investigation of WM microstructural biomarkers and endophenotypes in BD. The first whole-brain DTI studies generated heterogeneous results concerning the type of FA variation (increase or decrease) and the precise location of these changes. Some studies have reported a localized (Bruno *et al.*, 2008; Liu *et al.*, 2010; Sussmann *et al.*, 2009) or diffuse decrease in FA (Chan *et al.*, 2010; Kafantaris *et al.*, 2009; Zanetti *et al.*, 2009), whereas others have reported an increase in FA in diffuse regions (Michèle *et al.*, 2009) or a mixture of increases and decreases in FA (Mahon et al., 2009; Versace et al., 2008). This may reflect different

methodological approaches and heterogeneity within the clinical populations studied.

Review studies (Brambilla et al., 2009; Heng et al., 2010; Mahon et al., 2010; Sexton et al., 2009; Womer et al., 2009) and meta-analysis (Vederine *et al.*, 2011) of DTI studies in BD have tried to summarize the results, even if several issues are still unaddressed.

Gray Matter

A number of studies have examined structural gray matter characteristics in cortical and subcortical regions of adults with BD. Many of them was conducted by means of volumetric measurements of regional brain structures and the results often showed inconsistent findings (Arnone *et al.*, 2009; McDonald *et al.*, 2004b). Specifically, previous studies in BD patients have examined cortical regions implicated in emotion processing and cognitive processes that are important for emotion regulation, including the cingulate cortex as well as frontal and temporal regions (Lyoo *et al.*, 2004; Nugent *et al.*, 2006; Wilke *et al.*, 2004). Prefrontal cortical gray matter volumes had been found to decrease with illness progression (Kalmar *et al.*, 2009) but normalize (or even increase) with treatment (Moore *et al.*, 2000, 2009). Studies have also reported widespread decreases in frontal cortical thickness bilaterally, especially in the right hemisphere, and abnormally decreased temporal and parietal cortical thickness bilaterally in adults with

bipolar disorder (Foland-Ross *et al.*, 2011; Rimol *et al.*, 2010).

A second key finding relating to emotion processing and regulation neural circuits is decreased subcortical deep gray matter structures. Specifically, abnormally decreased hippocampal and parahippocampal volumes have been reported in adults with bipolar disorder (Almeida *et al.*, 2009; Rimol *et al.*, 2010; Wijeratne *et al.*, 2013), although such abnormalities may be masked or compensated by treatment (Foland *et al.*, 2008; Hajek, Kopecek, *et al.*, 2012; Hallahan *et al.*, 2011).

Although volumetric analyses of structural brain imaging data have been a mainstay of brain structure investigations in BD, in recent years methodological developments have led to structural measures that can supplement them. Specifically, recent studies in BD reported changes in shape of the surface of the caudate nucleus (Ong *et al.*, 2012), putamen, ventral striatum and thalamus (Womer *et al.*, 2014). Shape analysis enables the uncovering of localized deformations on the surface of a brain structure and it may more precisely identify impaired morphologies within the brain. This is particularly important in the study of brain structures with explicit regional differentiation in functions, such as thalamus or striatum (Herrero et al., 2002), that are central subcortical areas involved in BD (Womer *et al.*, 2014).

The variability of the results is still predominant in BD literature findings (McDonald *et al.*, 2004) and perhaps unsurprising given the enormous clinical heterogeneity (e.g. in illness subtype, mood-state, medication status, illness severity and duration, etc.) and small size of samples studied. For instance, one much debated source of bias in the study of brain volumetric associations with BD is the effect of mood-stabilizing medications, primarily lithium, which may influence brain structure (Hartberg et al., 2015; Hibar et al., 2016). Neuroimaging studies are promising components for a new diagnostic framework for BD, but a major issue is the potential confound of psychotropic medication upon experimental measures. Withdrawing all individuals from medication and examining only unmedicated individuals may be clinically unfeasible and may render findings less generalizable. Ideally, comparisons of medicated with unmedicated individuals should be included in cross-sectional functional neuroimaging studies of bipolar disorder.

The present work aimed to address these specific aspects. Specifically, study 1 investigated the trajectories of grey and white cerebral volumetry in bipolar disorder progressions, while study 2 and 3 assessed the impact of pharmacological treatment with lithium on subcortical structures volumetry and shape, respectively.

CHAPTER 2

Study 1: Gray and white matter trajectories in patients with bipolar disorder

2.1 Introduction

As stated above, although several structural abnormalities in the cortical, subcortical, and limbic systems of patients with bipolar disorder (BD) have been documented, the findings are often inconsistent. For example, gray matter (GM) volumes of several structures, including the cingulate cortex as well as frontal and temporal regions, have been found to be reduced (Lyoo *et al.*, 2004), to be increased (Adler *et al.*, 2007), or to show no differences (McDonald *et al.*, 2005) when compared with healthy control subjects (HC). Furthermore, two large meta-analyses of cross-sectional structural imaging studies of patients with BD also yielded inconclusive results. In particular, Kempton and colleagues (Kempton *et al.*, 2008) described increased brain ventricular volumes and corpus callosum atrophy, while Arnone and colleagues (Arnone *et al.*, 2009) found significant whole-brain and prefrontal lobe reductions. More recently, Selvaraj and collaborators (Selvaraj *et al.*, 2012) found neuroanatomical abnormalities

in the right prefrontal cortex, anterior cingulate cortex, insula, and claustrum in patients with BD. Some voxel-based morphometry (VBM) studies highlighted regional and global reductions in white matter (WM) volume and density (Chen *et al.*, 2004; Davis *et al.*, 2004), while others failed to replicate these findings (López-Larson *et al.*, 2002; Scherk *et al.*, 2008). This mirrors the lack of concordance found in GM studies.

Although longitudinal studies yielded more consistent findings of progressive atrophy of the prefrontal cortex, anterior cingulate cortex and subgenual region, they yet again reported less consistent findings for temporal and related regions, such as the hippocampus (Lim *et al.*, 2013). To understand which brain abnormalities are present from the very beginning of the disorder and to evaluate how they change during the illness course, it is fundamental to assess patients with BD over a long-time span. It is also necessary to have a long observational period to determine whether the ageing process affects patients with BD and HC differently. Thus, to address all these critical issues, this work employed a cross-sectional case-control study to compare structural brain abnormalities at different ages (hereafter called trajectories) in patients with BD and HC over a time period of about 50 years.

The primary aim of the present study was to understand whether WM and GM changes were present from the beginning of the illness and whether they

continued to be present over the course of the illness. Since patients with bipolar disorder types I (BD-I) and II (BD-II) have different symptomatology and severity, preliminarily we compared trajectories between the two subgroups to verify their homogeneity and investigate shared and unique diagnosis-related neuro-anatomical abnormalities.

2.2 Methods and Materials

The study was approved and undertaken in accordance with the guidelines of the Santa Lucia Foundation Ethics Committee. All participants gave their written informed consent to participate in the research after they had received a complete explanation of the study procedures.

G*Power statistical software (Erdfelder et al., 2009), was used to compute power analysis. Results shown that a sample size of at least 19 would have greater than 80% power to detect a difference between groups with an alpha value of <0.05 (two tailed).

Participants

Consecutive patients with a diagnosis of BD according to the Diagnostic and Statistical Manual of Mental Disorders IV-Edition, Text Revised (DSM-IV-TR)

(American Psychiatric Association, 2000) were assessed at the Santa Lucia Foundation in Rome, between January 2012 and January 2015. Inclusion criteria for all participants were: (i) age between 18 and 75 years, (ii) at least five years of education, and (iii) suitability for magnetic resonance imaging (MRI) scanning. Exclusion criteria were: (i) history of alcohol or drug abuse in the two years before the assessment, (ii) lifetime drug dependence, (iii) traumatic head injury with loss of consciousness, (iv) past or present major medical illness or neurological disorders, (v) any (for HC) or additional (for patients with BD) psychiatric disorder or mental retardation, (vi) dementia or cognitive deterioration according to DSM-IV-TR criteria, and Mini-Mental State Examination (MMSE) (Folstein *et al.*, 1975a) score < 25, consistent with normative data in the Italian population (Measso, G., Cavarzeran, F., Zappalà, G., Lebowitz, B. D., Crook, T. H., Pirozzolo, F. J., ... & Grigoletto, 1993), and (vii) any potential brain abnormality or microvascular lesion as apparent on conventional fluid attenuated inversion recovery (FLAIR) scans; in particular, the presence, severity, and location of vascular lesions were computed according to the semi-automated method recently published by Santa Lucia Foundation neuropsychiatric research (Iorio *et al.*, 2013).

All patients were recruited at three sites: the Lithium Clinic at Sant'Andrea Hospital, Villa Von Siebenthal, and the Santa Lucia Foundation in Rome. The clinical

psychiatrist who had been treating the patients and knew their clinical history, and who was blind to the aims of the study, made the preliminary diagnosis using the DSM-IV-TR criteria. All clinical diagnoses were confirmed by a research psychiatrist using the Structured Clinical Interview for DSM-IV-TR-Patient Edition (SCID-I/P) (First *et al.*, 2002). If the diagnoses made at the two different steps were not consistent, more data were gathered and the diagnostic process continued until a final diagnostic consensus was reached. If an agreement could not be reached, the patient was removed from the sample.

The researchers involved in the assessment of the patients completed an intensive training program in preparation. The training program consisted of bi- or tri-weekly eight-hour sessions where junior researchers assessed the patients under the continuous supervision of a senior researcher. The training program lasted from three to six months, and did not end until all the researchers were able to make a psychopathological and neuropsychological assessment achieving good inter-rater reliability ($k \geq 0.8$).

Eighty-five patients with BD were initially included in the present study. Of the original group of patients, three refused to undergo the MRI exam and four were excluded for the presence of moderate to severe brain vascular lesions (see exclusion criteria). The remaining sample of 78 patients included 49 with BD-I and 29 with BD-II.

We also recruited 78 HC in the same geographical area. They were carefully matched with the patients for age (2 years), gender, and educational level (2 years). All HC were screened for a current or lifetime history of DSM-IV-TR Axis I and II disorders using the SCID-I-NP) (First *et al.*, 2002) and SCID-II (M. B. First *et al.*, 1997); they were also assessed to confirm that no first-degree relative had a history of mood - or schizophrenia-related disorders.

The overall severity of affective symptoms was assessed using the 17-item Hamilton Depression Rating Scale (HDRS) (Hamilton, 1960) and the Young Mania Rating Scale (YMRS) (Young *et al.*, 1978). Age at onset was defined as 'age at onset of first affective symptoms', which were investigated in an interview with patients and first-degree relatives. All patients were under stable pharmacologic treatment for at least six months, usually polipharmacy, including treatment with antidepressants, mood-stabilizing agents, and stable oral dosages of one or more antipsychotics (data not shown; available upon request).

Image acquisition and processing

All 156 participants underwent the same imagingprotocol, which included 3D T1-weighted, T2-weighted and FLAIR sequences using a 3T AllegraMR imager (Siemens, Erlangen, Germany) with a standard

quadrature head coil. Whole-brain T1-weighted images were obtained in the sagittal plane using a modified driven equilibrium Fourier trans-form sequence (echo time/repetition: time=2.4/7.92msec, flip angle=15°, voxel size=19191mm3). T2 and FLAIR sequences were acquired to screen for brain pathology.

T1-weighted images were processed and examined using SPM8 software (Wellcome Department of Imaging Neuroscience Group, London, UK; www.fil.ion.ucl.ac.uk/spm) and specifically the VBM toolbox VBM8 (http://dbm.neuro.uni-jena.de/vbm.html) running in Matlab2007b (MathWorks, Natick, MA, USA). VBM8 extends the unified segmentation model (Ashburner and Friston, 2005) consisting of MRI field intensity inhomogeneity correction, spatial normalization and tissue segmentation at several pre-processing steps to further improve data quality. The segmented GM and WM maps were registered to the Montreal Neurological Institute (MNI) space using the iterative high-dimensional normalization approach provided by the Diffeomorphic Anatomical Registration Through Exponentiated Lie Algebra (DARTEL) (Ashburner, 2007) toolbox. The normalized tissue maps were written with anisotropic voxel resolution of 1.5 x 1.5 x 1.5 mm3. The tissue deformations were then used to modulate participants' GM and WM maps. Finally, the modulated and normalized GM and WM segments were smoothed with an 8-mm full-width half-

maxi-mum Gaussian kernel. The segmented, normalized, modulated and smoothed GM and WM images were used for analyses.

Statistical analyses

Comparisons between the diagnostic groups on sociodemographic characteristics (age, gender, and educational level) were performed using the t-test or chi-square test.

Factorial analysis of covariance (ANCOVA) was used to compare, at the voxel level, the potential age-related changes in terms of brain volume, evaluated in GM and WM, between diagnostic groups. For both tissues, volume was the dependent variable, and diagnosis was included as a fixed factor (independent variable), and age as a covariate. We did not include illness duration as a regressor in the ANCOVA model since it was strongly collinear with age (R=0.65) and the presence of collinear regressors could reduce the strength of results (Berk, 1977). We first verified the linear dependence between volume and age, the primary hypothesis of ANCOVA. Then, we verified the ANCOVA assumption of homogeneity of regression slopes, i.e., we looked for the absence of any interaction between diagnosis and age. Where this hypothesis was fulfilled, we looked for

the presence of a main effect of the diagnosis. To avoid type I errors (i.e., accepting false positives) all these analyses were performed using the family-wise error (FWE) correction ($p<0.05$), which controls for the possibility of any false positives across the entire volume (Ashburner and Friston, 2005). In addition, results were considered statistically significant if they were part of a spatially contiguous cluster of 30 voxels or greater. As already mentioned, we used the normalized and modulated images for the analysis, which already accounted for different head sizes in the data. Therefore, there was no need for further corrections for head size in the statistical model.

Before comparing age-related trajectories between the whole group of patients with BD and HC, we first determined whether there was any difference in the age-related trajectories followed by GM and WM volumes between the two subgroups of patients, i.e., those with BD-I and BD-II. In this case, the comparisons were performed at the significance level of $p<0.05$, uncorrected for multiple comparisons, in order to avoid type II errors (i.e., rejecting false negatives) in the final results. These groups were not different for age and gender, but were different for illness duration (Table 1) and we therefore included this continuous variable in the ANCOVA model to correct for its potential effect.

Table 1. Sociodemographic and clinical characteristics of patients with bipolar disorder

Characteristic	BP-I (n = 49)	BP-II (n = 29)	t or χ^2	df	p-value
Age, years, mean ± SD	43.71 ± 12.84	46.00 ± 14.05	−0.73	76	0.46
Males, n (%)	26 (53.06)	12 (41.37)	0.99	1	0.31
Educational level, years, mean ± SD	13.59 ± 3.84	14.58 ± 3.50	−1.14	76	0.25
Duration of illness, years, mean ± SD	15.12 ± 11.08	20.93 ± 13.17	−2.08	76	0.04

BP-I = bipolar I disorder; BP-II = bipolar II disorder; df = degrees of freedom; SD = standard deviation.

4.4 Results

Sociodemographic and clinical characteristics

Sociodemographic and clinical characteristics of the patients are shown in Tables 1 and 2. The youngest patient was 21 years old, and the oldest was 72 years old. Specifically, we had 13 patients in the 21–30 years age group, 20 patients in the 31–40 years age group, 15 patients in the 41–50 years age group, 21 patients in the 51–60 years age group, six patients in the 61–70 years age group, and three patients in the 71–75 years age group. The groups of patients with BD-I and BD-II and the group of HC did not significantly differ for age, gender, and educational level, but the BD-I and BD-II groups differed for illness duration.

Table 2. Sociodemographic and clinical characteristics of 78 patients with bipolar disorder (BP) and 78 healthy control subjects (HC)

Characteristic	BP (n = 78)	HC (n = 78)	t or χ^2	df	p-value
Age, years, mean ± SD	44.56 ± 13.26	44.38 ± 13.31	0.084	154	0.93
Males, n (%)	38 (48.71)	38 (48.71)	0.00	1	>0.999
Educational level, years, mean ± SD	13.96 ± 3.73	14.27 ± 3.15	−0.557	154	0.58
Bipolar I disorder, n (%)	49 (62.82)				
Duration of illness, years, mean ± SD	17.28 ± 12.15				
Current mood phase					
MDE, n (%)	41 (52.5)				
Euthymia, n (%)	29 (37.1)				
(Hypo)mania, n (%)	5 (6.4)				
DSM-IV-TR mixed state, n (%)	3 (4.0)				
HDRS score, mean ± SD	11.56 ± 8.59				
YMRS score, mean ± SD	5.05 ± 6.41				
Current pharmacotherapy, n (%)[a]					
Antipsychotics	49 (65.33)				
Lithium	45 (60)				
Antiepileptics	39 (52)				
Benzodiazepines	33 (44)				
Antidepressants	23 (30.66)				

df = degrees of freedom; HDRS = Hamilton Depression Rating Scale; MDE = major depressive episode; SD = standard deviation; YMRS = Young Mania Rating Scale.
[a]Analysis performed on 75 patients.

Age-related gray matter trajectories

When comparing age-related GM trajectories between patients with BD-I and BD-II, we did not find GM voxels with either a significant interaction between diagnosis and age or a main effect of diagnosis, indicating that the age-related GM trajectories of both patient subgroups were indistinguishable for all GM voxels. We therefore analyzed the two BD subtypes as one group and continued comparing age-related trajectories between patients with BD and HC. In the ANCOVA comparing patients with BD and HC, the test for voxel-wise linear dependence between GM volume and age revealed a negative linear correlation ($p<0.05$) in clusters distributed in the entire GM in both BD and HC. While no interaction between diagnosis and age emerged, the ANCOVA analysis unveiled a significant ($p<0.05$,

FWE-corrected) main effect of diagnosis in four clusters. As shown in Figure 1 and described in Table 3, one cluster was localized in the posterior cingulate cortex (PCC), one in the right thalamus and two clusters were localized bilaterally in the cerebellum. In order to identify which thalamic area the cluster in the thalamus belonged to, we employed the probabilistic thalamic Connectivity Atlas (Johansen-Berg *et al.*, 2004) (http://www.fmrib.ox.ac.uk/connect) that divides the thalamic structure according to the projections to different cortical regions, and it emerged that the whole cluster belonged to the thalamic area projecting to the temporal lobe.

Analogously, to obtain the precise anatomical localization of clusters in the cerebellum, we superimposed our results onto Diedrichsen's probabilistic atlas, which subdivides the cerebellum into 10 different regions (Diedrichsen *et al.*, 2009), and it appeared that the cerebellar clusters belonged bilaterally to lobules I–IV (see Table 3). In particular, the ANCOVA results suggested that the GM age-related trajectories of the two diagnostic groups were parallel (no interaction) and that they were significantly different starting from the youngest age (main effect of diagnosis). To confirm this, we calculated the mean GM intensity for each subject in those regions where an effect of diagnosis emerged and plotted the mean GM intensity as a function of age for the two groups. As shown in Figure 1,

the patients had reduced GM with respect to HC in the entire age range considered. In each cluster, the slopes of the linear regressions fitting the data of the two diagnostic groups were significant ($p<0.05$) and, as the absence of interaction between diagnosis and age suggested, statistically indistinguishable.

Table 3. Gray matter clusters where a main effect of diagnosis emerged

Anatomical region	Cluster extent	p (FWE-corrected)	*Z*-score	Coordinates of the statistical peak		
				x	y	z
Bilateral posterior cingulate cortex (BA 23)	1058	<0.001	5.69	6	−25	39
		0.001	5.19	2	−36	30
		0.019	4.47	2	−54	15
Left cerebellum (lobule I–IV)	669	<0.001	5.85	−6	−42	−20
		<0.001	5.49	−12	−49	−12
Right cerebellum (lobule I–IV)	110	<0.001	5.46	9	−42	−21
Right thalamus	52	<0.05	5.08	1	−7	9

BA = Brodmann's area; FWE = family-wise error.

Fig. 1. Significant effect of diagnosis in gray matter changes. **Top:** F-maps of gray matter clusters with a significant effect of diagnosis (sagittal and axial views). **Bottom:** age-related gray matter trajectories for patients with bipolar disorder (blue dots) and healthy control subjects (yellow dots). Continuous lines have been added for visualization purposes. z coordinates are in Montreal Neurological Institute space. L = left; R = right.

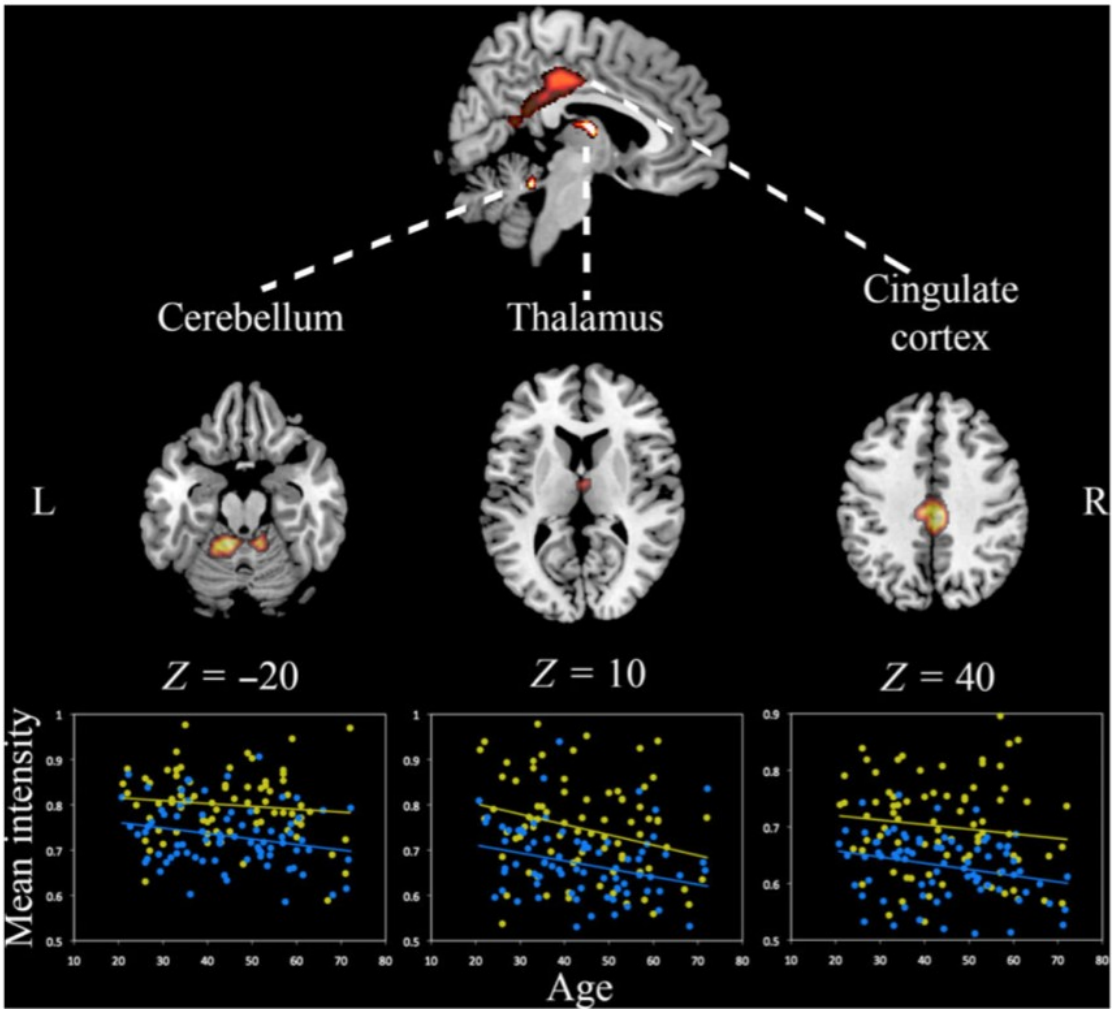

Age-related white matter trajectories

In accordance with results found in GM, WM trajectories of patients diagnosed with BD-I and BD-II were indistinguishable for all WM voxels. Therefore, we compared age-related trajectories between the whole BD group and HC. We first tested for the voxelwise linear

dependence between whole-brain WM and age inpatients with BD and HC, and we found a negative correlation ($p<0.05$) in both groups for all WM voxels. While no interaction between diagnosis and age emerged, the ANCOVA revealed a main effect of diagnosis in one cluster [1,242 voxels, Z-score=5.18, p (FEW-corrected) <0.0001] with the statistical peak localized in the left posterior limb of the internal capsule (MNI coordinates: x=-26, y=-13, z=-2) (see Fig. 2). In particular, the ANCOVA results indicated that the WM age-related trajectories of the two diagnostic groups were parallel (no interaction) and that they were significantly different starting from the youngest age (main effect of diagnosis). Figure 2 shows that patients had reduced WM with respect to HC in the whole age range considered. The fitted linear regressions were both significant ($p_{BD}=0.006$ and $p_{HC}=0.02$), Pearson's correlations were $r_{BD}=-0.31$ and $r_{HC}=-0.26$, and the slopes were $slope_{BD}=-0.0017$ and $slope_{HC}=-0.0013$).

Fig. 2. Significant effect of diagnosis in white matter changes. **Top:** F-maps of white matter clusters with a significant effect of diagnosis. **Bottom:** age-related white matter trajectories for patients with bipolar disorder (blue dots) and healthy control subjects (yellow dots). Continuous lines have been added for visualization purposes. x, y, z coordinates are in Montreal Neurological Institute space. Coordinates and related anatomical views here reported (but not the correlation graph calculated on the entire cluster) are different from those of the statistical peak to improve the visualization of anatomical areas involved. L = left; R = right.

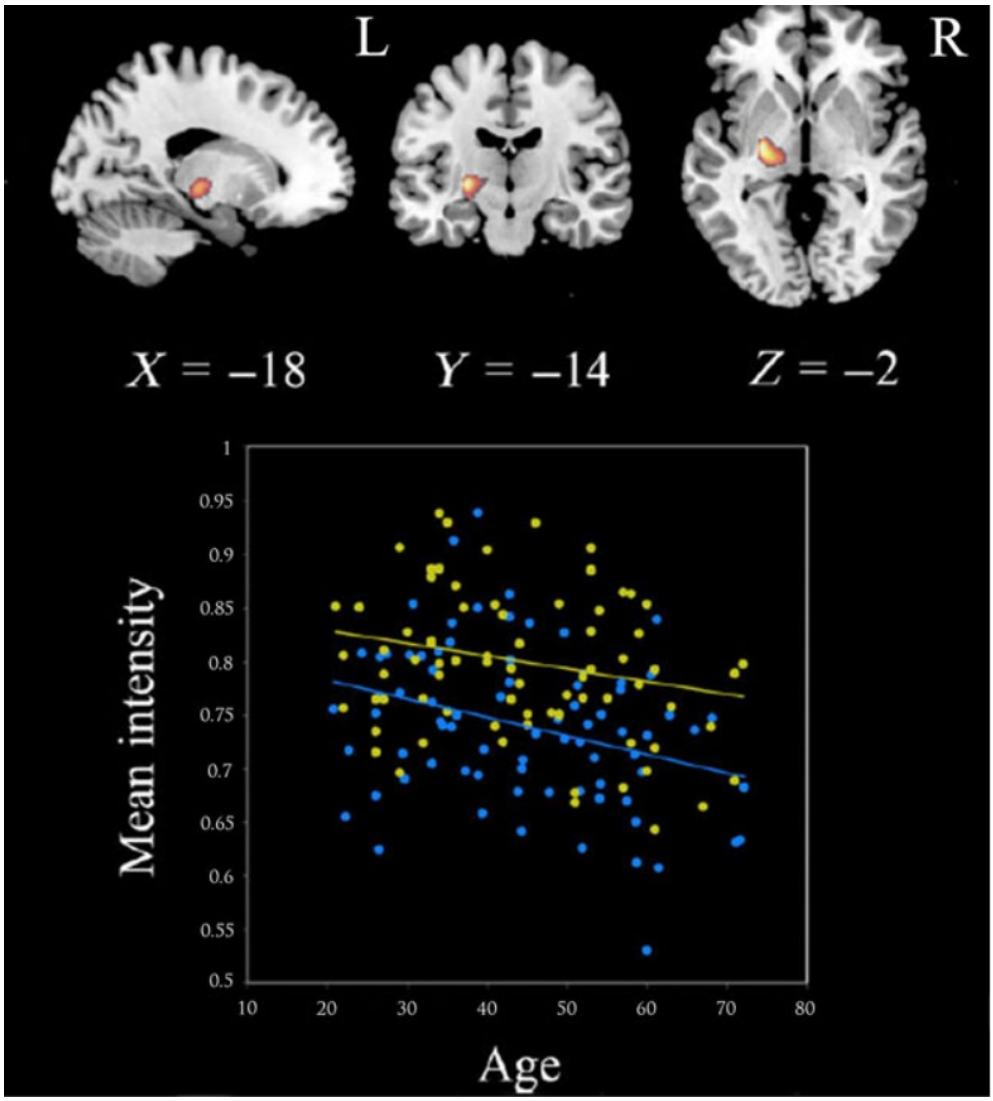

2.4 Discussion

The aim of this study was to investigate the presence of structural brain abnormalities at different ages in patients affected by BD and to compare them to those in HC. The present work was based on cross-sectional case–control comparisons.

Previous studies have already used a cross-sectional design to evaluate brain modifications over a span of time in patients diagnosed with schizophrenia (Chiapponi *et al.*, 2014), BD (Lopez-Larson *et al.*, 2010), major depressive disorder (Hagan *et al.*, 2015), and autistic spectrum disorder (Greimel *et al.*, 2013). Our results revealed age-related atrophy in GM and WM volumes in both patients and HC, as already found in a previous large study focused on patients with BD-I in the euthymic phase (Emsell *et al.*, 2013). With respect to HC, patients with BD showed a reduced brain volume in areas comprising the PCC (BA23) bilaterally, the right thalamus, the bilateral cerebellum and the left posterior limb of the internal capsule. The fact that these areas were permanently reduced over the entire age range investigated here suggests that brain alterations are present from the very early phase of the disorder, and that the brain alterations are not the results of a neurodegenerative process.

All cerebral areas where a main effect of diagnosis was found are involved in the regulation of two important

dimensions in BD: mood/emotion and psychomotricity. The PCC plays a central role in the default mode network (DMN) (Buckner *et al.*, 2007). PCC and DMN abnormalities are present in a wide range of neurological and psychiatric disorders (Buckner *et al.*, 2007; Leech and Sharp, 2014), including mood disorders. Specifically, several MRI studies have reported abnormal functional activity in major depression, although the abnormalities reported are variable (Berman *et al.*, 2011; Bluhm *et al.*, 2009; Zhou *et al.*, 2010; Zhu *et al.*, 2012). Studies on patients with BD are still scarce and results are inconsistent. Compared to HC, volumes of PCC in patients with BD were found to be increased (Adler *et al.*, 2007), unchanged (Sassi *et al.*, 2004) or decreased (Atmaca *et al.*, 2007; Kaur *et al.*, 2005). Consistent with the findings of a previous report (Kaur *et al.*, 2005), here we found that the volume of the PCC was decreased from the very early phase of the disease.

The thalamus, a fundamental relay station that connects cortical and subcortical structures as well as different cortical regions, has been reported to be functionally involved in the modulation of emotions, cognition and social behavior (Strakowski *et al.*, 2005). There is an important heterogeneity in the findings of thalamic volume alterations in patients with BD (Ng *et al.*, 2009). To summarize, the majority of studies reported no significant volumetric or GM thalamic differences in patients with BD

compared to HC, while few other studies found either increased or decreased thalamic volume. Our data are in line with the latter studies. In particular, we found a volume reduction in the thalamic area projecting to the temporal pole, hippocampal formation, and amygdala (Behrens *et al.*, 2003). It is noteworthy that these structures are part of the limbic system, a group of interconnected are as that classically have been thought to be involved in control of emotions and episodic memory. Recently, a new model of the limbic system has been proposed and it was noted that the alterations of the temporo-amygdala-orbitofrontal network are often present in patients affected by several psychiatric conditions (Catani *et al.*, 2013). According to present findings, it is possible to hypothesize that these alterations in patients with BD are associated with abnormalities in that specific thalamic subregion.

Our findings involving the cerebellum are intriguing, considering its role in the regulation of mood and emotions. Both structural and functional abnormalities were found in the cerebellum of psychiatric patients (Hoppenbrouwers *et al.*, 2008). Reduced volumes of the vermis and other cerebellum abnormalities have been found in patients affected by BD (Hoppenbrouwers *et al.*, 2008; Kim *et al.*, 2013; Mills *et al.*, 2005), even though a recent study did not confirm this result (Laidi *et al.*, 2015). We found a decreased volume of the anterior cerebellar lobules, which are primarily involved in the motor control system.

Although BD is classified as an affective disorder, psychomotor alterations are classic clinical signs (Kraepelin, 2014), present in different phases of the disease, and the focus of clinical (Parker *et al.*, 1994; Sani *et al.*, 2014), neuropsychological (Bora *et al.*, 2007) and neurobiological investigations (Liberg *et al.*, 2014; Walther *et al.*, 2012). In contrast to a previous report (Kim *et al.*, 2013) describing how the damage to the posterior cerebellar regions appears to progress over the course of illness (but could potentially be delayed and/or reversed by appropriate pharmacological treatment), in our sample, the reduction of volume was present from the beginning and remained stable during the course of the illness. This suggests that the reduction of cerebellar volume is due to the illness and, following pharmacological treatment, remains stable over time. However, an apparent independence of cerebellar volume from pharmacological treatments, such as lithium or antipsychotics, was found in a recent large international study (Laidi *et al.*, 2015). In the WM context around the thalamus, we found a decreased density of the WM fibers of the posterior limb of the internal capsule. The posterior limb of the internal capsule mostly includes the fibers of the corticospinal tract (CST), which contains ascending fibers from the thalamus to the cerebral cortex and descending fibers from the fronto-parietal cortex to the subcortical nuclei and spinal cord. It conveys information among primary and secondary motor areas, the thalamus, the

prefrontal cortex and the cerebellum. Moreover, this system is involved both in motor functions and in cognition and emotional regulation in individuals at high genetic risk for (Sprooten *et al.*, 2011) or in the early phase of BD (Lu *et al.*, 2011). Alterations of the CST were found in previous DTI studies, although the results are inconsistent (Mahon *et al.*, 2009; Paillère Martinot *et al.*, 2014). In any case, our data confirm that the CST is involved in the mechanisms of BD and suggest that the alteration of the CTS may be considered as part of the more general WM connectivity alterations found in patients with BD (Mahon *et al.*, 2010).

It is intriguing that all the cerebral areas showing a volume reduction are part of the two main brain networks involved in regulation of mood and emotions: the limbic-thalamic-cortical circuit, which includes part of the thalamus, the medial and ventrolateral prefrontal cortex, and the limbic-striatal-pallidal-thalamis cortical circuits, which include the striatum, the ventral pallidum, and the regions of the former circuit (Soares and Mann, 1997). The cerebellum is part of these networks projecting to several structures of the brainstem and limbic system, such as the amygdala, hypothalamus, hippocampus, and septum. Thus, we identified critical areas, part of the brain networks devoted to mood and motor control, which had structural alterations from the very early phase of the disorder. These abnormalities in the brain circuits may be the expression of a biological vulnerability, or the precocious signs of the

disorder. Hence, it is plausible to believe that these areas play an early role in the mechanism of BD. Taken together, our findings add an important piece to the complex puzzle of the mechanism of BD. In fact, in contrast with other severe psychiatric disorders, in particular schizophrenia, where a possible pathogenesis related to neurodevelopmental disruption is supported by classical neurodevelopmental models (Fatemi and Folsom, 2009; Lewis and Murray, 1987; Weinberger, 1987), it is still uncertain whether neurodevelopment is implicated in the physiopathology of BD. It is possible that environmental factors, especially early traumatic factors, may interplay with a specific genetic susceptibility, affecting the clinical characteristics of the disorder (Janiri *et al.*, 2015) as well as altering the development of specific brain areas and leading to inadequate mood regulation (Etain *et al.*, 2008). In fact, while other authors suggested that the decrease of GM volumes may be a neurodegenerative effect due to the course of the disease (Frey *et al.*, 2008), we found that the structural alterations did not change over the course of the disorders. This strengthens the idea that they may be a signature of the disorder, if not real endophenotypes of BD.

Finally, in a preliminary analysis, as already stated, we compared patients with BD-I and BD-II to determine whether to consider them as one singular group or two separate groups. Notably, we found that their age-related GM and WM trajectories were indistinguishable. Beyond

the clinical phenomenology, there is still a dearth of neurobiological data on the difference between BD-I and BD-II, and findings from pathophysiological and neuroimaging studies are still not consistent (Vieta and Suppes, 2008). Our findings do not support the current division between the two types of BD based on the presence of mania or hypomania, at least according to the brain structural data here considered.

2.5 Limitations

Before concluding, we should mention several issues potentially limiting the generalizability of our results. Our findings suggest a neurodevelopmental pathogenesis for BD. We know that each brain structure has its own developmental trajectory (Giedd *et al.*, 1999) and that illness may affect it. Patients with BD and HC showed differences in both GM and WM structures already at the age of 21 years, i.e., the lowest age we could recruit. We cannot know how such differences developed before that age, but we know that they started at an earlier age. Alterations could have been present at any time before that age and may even have started before the onset of the illness. Another consideration is that all our patients were on medication, often on polypharmacy, as usually happens in the pharmacological treatment of patients with severe illness

(Centorrino *et al.*, 2005). To identify age-related changes, it would be desirable to follow up patients over time using longitudinal study designs. However, this would be unethical in untreated patients. To overcome this hurdle, it is possible to draw some conclusions about changes occurring with time by comparing different age ranges in a sample of adult patients with BD. However, the neurobiology of late-onset BD in drug-naïve patients may differ from that of the most common, early-onset BD (Oostervink *et al.*, 2015). Longitudinal studies may investigate better than cross-sectional studies any change with time, with each patient representing his/her own control. How-ever, this would entail a considerable economic effort and would carry the risk of increased patient/control drop-out, thus necessitating the inclusion of a higher number of subjects to avoid the study being underpowered. This is why studies with more than 10 years of follow-up in BD are lacking. In spite of the intrinsic limitations of cross-sectional designs, such designs may yield reliable, real-world, results if sufficiently powered. Furthermore, we cannot exclude a neuroprotective role of drug treatment that prevented increased neurodegeneration from occurring. Moreover, we did not find any difference in GM and WM age-related trajectories between patients with BD-I and BD-II. Given the small number of patients with BD-II (n=29), we cannot rule out the possibility that this lack of difference may have been attributable to insufficient

statistical power. However, that risk was minimized by the fact that we were focused on type II error and the comparisons were performed at a significance level of $p<0.05$ uncorrected for multiple comparisons. Finally, our clinical sample consisted of patients with BD without other comorbidities. Although, on the one hand, this may limit the generalizability of our findings, on the other hand it increases their reliability.

CHAPTER 3

Study 2: Association between Duration of Lithium Exposure and Hippocampus/Amygdala Volumes in Type I Bipolar Disorder

3.1 Introduction

Limbic and subcortical structures are involved in emotional generation, expression, experience, and regulation (Phan et al., 2002) and are structurally and functionally altered in individuals with mood disorders (i.e., bipolar disorder [BD], major depressive disorder [MDD]) and psychotic disorders (Phan *et al.*, 2002). A growing body of histological (Gigante *et al.*, 2011; Hercher *et al.*, 2009) and magnetic resonance imaging (MRI) (Graham *et al.*, 2013; Janiri *et al.*, 2017; Phillips and Swartz, 2014) findings suggest that the amygdala and hippocampus, in particular, are structurally altered among persons with BD. However, MRI studies of these structures in BD are discrepant with respect to the direction and magnitude of such alterations, with larger (Altshuler *et al.*, 1998; van Erp *et al.*, 2012; Hallahan *et al.*, 2011) smaller (Almeida *et al.*, 2009; Bearden *et al.*, 2008; Haller *et al.*, 2011; Ong *et al.*, 2012;

Rimol *et al.*, 2010; Wijeratne *et al.*, 2013) or unaltered (Arnone *et al.*, 2009; Kempton *et al.*, 2011; McDonald *et al.*, 2004) hippocampal and amygdalar volumes reported when persons with BD are compared to healthy controls (HC).

Some authors hypothesized that these inconsistencies are due to the effect of psychotrophic medications, some of which may alter the volumes of some brain structures (Hafeman *et al.*, 2012; Hajek *et al.*, 2012b). Pre-clinical (McDonald *et al.*, 2015; Quiroz *et al.*, 2010) and clinical studies suggest that treatment with lithium–an agent that has been used for more than 70 years in the treatment of BD (A.H., 2006) – alters brain structure, especially limbic and subcortical structures (Bearden *et al.*, 2008; Foland *et al.*, 2008; Germaná *et al.*, 2010; Hajek, Cullis, *et al.*, 2012a; Hibar *et al.*, 2016; Radenbach *et al.*, 2010; Savitz *et al.*, 2010; Usher *et al.*, 2010). Indeed, hippocampal and amygdalar volumes are larger in lithium-treated patients than non-treated patients (Foland *et al.*, 2008; Germaná *et al.*, 2010), and the volumes of these structures are larger (Usher *et al.*, 2010) or unchanged (Bearden *et al.*, 2008; Hajek, Cullis, *et al.*, 2012a) in lithium-exposed patients when compared to HC. These observations prompted hypotheses regarding potential neuroprotective effects of lithium (Hajek, Kopecek, *et al.*, 2012), but inconsistencies in the observed effects of lithium on the direction and magnitude of lithium-related changes in limbic and

subcortical structures (using MRI-based techniques) has not yielded scientific consensus on this matter (Chepenik *et al.*, 2009; Doty *et al.*, 2008; Kempton *et al.*, 2009; Rimol *et al.*, 2010).

One possible explanation for these inconsistencies is that failure of most studies to consider possible time-dependent effects of lithium on the volumes of brain structures. Preclinical evidence suggests that the short-and long-term effects of lithium on neurons differ (Dixon and Hokin, 1998). Consistent with preclinical findings, MRI-based volumetric studies in humans are mixed with respect to the short-term effects of lithium on hippocampal volumes (Monkul *et al.*, 2007; A. Simonetti *et al.*, 2016; Yucel *et al.*, 2008) but relatively consistent with respect to the association between long-term lithium intake and larger hippocampal volumes in BD (Hajek, Kopecek, *et al.*, 2012; A. Simonetti *et al.*, 2016). The majority of studies that focused on the amygdala in BD have not evaluated the effects of duration of lithium exposure (Doty *et al.*, 2008; Foland-Ross *et al.*, 2012; Rimol *et al.*, 2010; Savitz *et al.*, 2010), but there is within these studies a suggestion of an association between long-term lithium treatment and larger amygdalar volumes (Germaná *et al.*, 2010; Hartberg *et al.*, 2015; Selek *et al.*, 2013). The effect of lithium on subcortical volumes is not well established and findings reported to-date are conflicting with respect to influence of lithium-treatment duration on thalamic, pallidal, putaminal,

and nucleus accumbens volumes (Abramovic *et al.*, 2016; López-Jaramillo *et al.*, 2017) or no effects (Brambilla *et al.*, 2001; Ong *et al.*, 2012; Quigley *et al.*, 2015).

Accordingly, the aim of this study was to investigate the effects of lithium-treatment duration on the volumes of limbic and subcortical structures by comparing four groups: BD type I (BD-I) naïve to lithium treatment, BD-I with short-term lithium treatment, BD-I with long-term lithium treatment, and HC. Based on the extant literature on limbic and subcortical volumes in BD-I - with the illness being associated with smaller limbic structure volumes and lithium treatment associated with larger volumes of these structures - the present study tested the hypothesis that long-term lithium treatment was associated with larger limbic and subcortical volumes when compared to short-term or no lithium treatment. Moreover, it was hypothesized that limbic and subcortical volumes would not differ between long-term lithium-treated patients and HC.

3.2 Methods and Materials

The study was approved by the Santa Lucia Foundation Ethics Committee and undertaken in accordance with the guidelines of the Helsinki Declaration of 1975. All participants gave their written informed consent to

participate in the research after they had received a complete explanation of the study procedures.

To be sure about the group representability, a power analysis was performed using G*Power statistical software (Erdfelder *et al.*, 2009). Results revealed that a total sample size of at least 27 subjects would have greater than 80% power to detect a difference between groups, with an alpha value of <0.05 (two tailed).

Participants

Seventy individuals with a diagnosis BD-I according to the DSM-IV-TR criteria (American Psychiatric Association, 2000) were recruited from the Sant'Andrea outpatient lithium clinic and the ambulatory of neuropsychiatry of the IRCCS Santa Lucia Foundation in Rome, Italy, and subsequently assessed at the Laboratory of Neuropsychiatry of the Santa Lucia Foundation in Rome, Italy.

Inclusion criteria were: 1) a diagnosis of BD-I; 2) age between 18 and 65 years; 3) at least five years of education; and 4) suitability for MRI scanning. Exclusion criteria were: 1) lifetime substance dependence or history of substance abuse in the one-year period before the assessment; 2) any (for HC) or additional (for patients) Axis I or Axis II disorders; 3) any neurological disorders; 4) suspicious of dementia or cognitive impairment based on a Mini-Mental State Examination (MMSE) (Folstein *et al.*, 1975b) score

lower than 25, consistent with normative data in the Italian population (Measso *et al*., 1993), or a diagnosis of dementia according to DSM-IV-TR (American Psychiatric Association, 2000) criteria confirmed by a clinical neuropsychological evaluation using the Mental Deterioration Battery (Carlesimo *et al.*, 1996); 5) major medical illnesses, e.g., diabetes, obstructive pulmonary disease or asthma, hematological and oncological disorders, pernicious anemia, significant gastrointestinal, renal, hepatic, endocrine, or cardiovascular system diseases, newly treated hypothyroidism; and 6) any potential brain abnormality or microvascular lesion as apparent on conventional FLAIR images. In particular, we imputed the presence, severity and location of vascular lesions according to the semi-automated method published by our group (Iorio *et al.*, 2013).

Initial BD-I diagnoses of potential participants were made by their treating psychiatrists, who provided the investigators with all available clinical information on the potential participants' past and current medical histories. A senior study psychiatrist then performed confirmatory diagnostic using the DSM-IV-TR Axis I disorders (SCID-I) (First *et al.*, 2002) and the Structured Clinical Interview for DSM-IV Axis II personality disorders (SCID-II) (First *et al.*, 1997). When diagnostic disagreement occurred between the treating and study psychiatrists, additional information needed to establish a consensus was obtained. When

diagnostic disagreement persisted despite such efforts, the participant was excluded from the sample.

From the initial sample, 25 patients were excluded due to the above-mentioned exclusion criteria. The remaining 45 patients were further divided in three groups according with the duration of lithium exposure: 15 patients with a lithium exposure of 24 or more months (long-exposure group [LE]), 15 patients with a lithium exposure of less than 24 months (short-exposure group [SE]), and 15 patients naïve to treatment with lithium (no-exposure group [NE]). Forty-seven out of sixty (78%) subjects of this sample were previously enrolled in another study that assessed the effect of lithium on the hippocampal subfields (A. Simonetti *et al.*, 2016). These participants were here selected with the purpose of creating three groups without differences in either clinical variables (i.e. duration of illness, number of episodes, current mood state) and/or past and current exposure to pharmacotherapies (i.e. antipsychotics, antidepressants, benzodiazepines, mood stabilizers other than lithium).

Twenty-four months was chosen as a cut-point for dividing duration of lithium treatment into short-and long-term categories based on our prior study of the association between duration of lithium exposure on hippocampal subfield volumes in patients with BD-I (A. Simonetti *et al.*, 2016). This categorization of duration of lithium treatment also is consistent with those in prior reports demonstrating

alterations in limbic cortical volumes associated with longer-term lithium exposure (van Erp *et al.*, 2012; Hajek, Cullis, *et al.*, 2012; Yucel *et al.*, 2007).

In the BD-I groups of the present study, depressive and manic symptoms were evaluated using the 17-item Hamilton Depression Rating Scale (HAM-D) (Hamilton, 1960) and the Young Mania Rating Scale (YMRS) (Young *et al.*, 1978), respectively. For the lithium-treated subgroups, the hypothesized effects of lithium treatment required an assumption of continuous exposure. Assessment of lithium exposure was made by review of clinical data provided by each participant's treating psychiatrist(s)and general practitioner(s).

Fifteen HC were assessed using the SCID-I (First *et al.*, 2002a) (First et al., 2002a) and SCID-II (First *et al.*, 1997) in order to exclude any Axis I or Axis II disorder or any major mental disorders in their first-degree relatives. The study exclusion criteria for patient groups were also applied to potential HC participants.

Image acquisition and processing

Each participant underwent whole-brain T1-weighted imaging using a 3T Allegra™ MR system (Siemens, Erlangen, Germany) with a standard quadrature head coil. Whole-brain T1-weighted images were obtained in the sagittal plane using a modified driven equilibrium Fourier

transform (MDEFT) sequence (TE/TR = 2.4/7.92 ms, flip angle 15o, voxel-size 1 × 1 × 1 mm3) (Deichmann *et al.*, 2004).

Limbic and subcortical volumes were determined using the automated procedure for volumetric measures of brain structures implemented in FreeSurfer 5.1 (https://surfer.nmr.mgh.harvard.edu) installed on a CentOS Linux 6.4. The automated procedure of subcortical volume segmentation has been described previously (Fischl *et al.*, 2002). Intracranial volume (ICV), that includes biological material such as meninges and cerebrospinal fluid in addiction to brain tissue, was calculated to correct the regional brain volumes analyses (Buckner *et al.*, 2004). Specifically, we corrected the volume of each subcortical structure for ICV according to the proportion method (Sanfilipo *et al.*, 2004).

Statistical analyses

The four study groups were compared for socio-demographic and clinical characteristics. Chi-Square test was used for nominal variables (i.e. gender, current mood state and past and current pharmacotherapy), while one-way analysis of variance (ANOVA) was applied for continuous variables (i.e., age, years of education, duration of illness, number of episodes, lithium exposure, YMRS and HAM-D scores).

Tests for differences in volumes of limbic (i.e. amygdala, hippocampus) and subcortical (i.e., caudate, hippocampus, nucleus accumbens, pallidum, putamen, thalamus) structures between the four study groups were performed using ANOVA, with diagnosis as independent variable and subcortical volumes as dependent variables. The Fischer's PLSD test was used for pairwise post-hoc comparisons for volumes that were found significantly different among groups. An alpha level of < 0.05 was used for comparative tests of significance, to which Bonferroni adjustment for multiple comparisons was then applied ($p< (0.05/14) = 0.0036$).

3.3 Results

Sociodemographic and clinical characteristics

The four study groups did not differ with respect to age, sex, and educational level. Furthermore, the three BD-I groups (NE, SE, LE) did not differ in terms of duration of illness, number of past episodes, current mood state, HAM-D scores, YMRS scores, or - with the exception of lithium exposure - current and past pharmacotherapies.

Limbic and subcortical gray matter structure volumes

One-way ANOVAs demonstrated an overall effect of duration of lithium treatment by group on bilateral amygdalar and bilateral hippocampal volumes as well as on the right nucleus accumbens (see table 2). The bilateral effect of lithium treatment on amygdalar and hippocampal volumes survived Bonferroni correction for multiple comparisons but the effect on the right nucleus accumbens did not. There were no between-group effects of duration of lithium treatment on caudate, putamen, pallidum thalamus and left accumbens volumes.

Post-hoc comparisons were performed to test for hypothesized specific between-group differences revealed significantly larger bilateral amygdalar and hippocampal volumes among both LE and HC when compared to NE. Amygdalar volumes were larger bilaterally in SE when compared to NE but did not differ from LE and HC. Hippocampal volumes were smaller bilaterally in SE when compared to LE and HC but did not differ from NE. Post-hoc comparisons did not yield differences in amygdalar or hippocampal volumes between LE and HC.

Table 1. Sociodemographic and clinical characteristics of study participants.

Characteristics	NE (N=15)	SE (N=15)	LE (N=15)	HC (N=15)	F or χ^2	df	*p*
Age (years), mean ± SD	41.10±13.41	42.80±12.22	43.22±11.96	42.93±8.81	0.10	3	0.96
Males, n (%)	8 (53.33)	8 (53.33)	8 (53.33)	8 (53.33)	>0.001	3	>0.99
Educational Level, (Years) mean ± SD	13.80±4.49	13.40±4.34	14.93±3.26	14.47±2.21	0.48	3	0.70
Duration of illness, (years) mean ± SD	15.33±11.41	13.00±12.76	16.33±7.59	-	0.37	2	0.69
Number of past episodes:							
Depressive, mean ± (SD)	2.47±1.19	3.53±2.10	3.87±2.72	-	1.82	2	0.17
Manic, mean ± (SD)	1.87±1.36	2.93±2.15	3.8±2.88	-	3.06	2	0.07
Mixed, mean ± (SD)	0.47±0.91	0.60±1.59	0.47±0.64	-	0.70	2	0.93
Hypomanic, mean ± (SD)	0.67±0.93	0.47±1.30	0.93±1.49	-	0.52	2	0.60
Current mood state:							
Euthymia, n (%)	4 (26.67)	9 (60.00)	8 (53.33)	-			
Depression, n (%)	7 (46.67)	5 (33.33)	3 (20.00)	-	5.60	4	0.23
Mania/mixed n (%)	4 (26.67)	1 (6.67)	4 (26.67)	-			
HAM-D, mean ± (SD)	10.13±7.78	7.20±8.35	4.73±3.69	-	2.28	2	0.11
YMRS, mean ± (SD)	6.47±8.10	3.93±4.73	6.93±6.67	-	0.89	2	0.42
Lithium exposure (months), mean ± SD	-	15.33±7.13	87.07±28.26	-	90.85	1	<0.001
Past pharmacotherapy							
Antidepressants, n (%)	8 (53.33)	8 (53.33)	8 (53.33)	-	<0.001	2	>0.99
Antipsychotics, n (%)	13 (86.66)	15 (100.00)	15 (100.00)	-	4.18	2	0.12
Antiepileptics, n (%)	12 (80.00)	12 (80.00)	13 (86.66)	-	0.30	2	0.86
Benzodiazepines, n (%)	7 (40.00)	7 (46.66)	10 (53.33)	-	0.26	2	0.88
Current pharmacotheraphy							
Antidepressants, n (%)	5 (33.33)	2 (13.33)	4 (26.67)	-	1.68	2	0.41
Antipsychotics, n (%)	12 (80.00)	10 (66.67)	10 (66.67)	-	0.86	2	0.64
Antiepileptics, n (%)	7 (46.67)	9 (60.00)	6 (40.00)	-	1.24	2	0.54
Benzodiazepines, n (%)	7 (46.67)	5 (33.33)	3 (20.00)	-	2.45	2	0.30

BP-I: Type I bipolar disorder; NE: patient with BP-I naïve to treatment with lithium; SE: patient with BP-I and exposure to lithium <24 months; LE: patient with BP-I and exposure to lithium >24 months; HC: healthy control; HAM-D: Hamilton Rating Scale for Depression; YMRS: Young Mania Rating Scale; df: degrees of freedom. SD = standard deviation.

Table 2 Deep gray matter structure volumes (mm3) of 45 BP-I patients with different lithium exposure and 15 HC

Anatomical region	Side	Mean (SD) mm3				F	df	*p* (Bonferroni-corrected)
		NE (N=15)	SE (N=15)	LE (N=15)	HC (N=15)			
ANOVA								
Amygdala	Right	10.1 (0.75)	11.73 (1.80)	11.29 (1.29)	11.99 (1.52)	5.57	3	**0.002**
	Left	9.09 (0.93)	10.94 (1.50)	10.94 (2.0)	10.69 (1.14)	5.7	3	**0.002**
Hippocampus	Right	23.95 (1.94)	24.22 (3.45)	26.26 (1.89)	27.37 (2.59)	6.22	3	**0.001**
	Left	23.33 (1.82)	23.35 (3.50)	25.21 (1.79)	26.57 (2.60)	5.78	3	**0.002**

ANOVAs were performed on total subcortical volumes corrected for intracranial volume (ICV). Significant p-values ($p < 0.05$) are indicated in bold. BP-I = Type I bipolar disorder; NE: patient with BP-I naïve to treatment with lithium; SE = patients with BP-I exposed to lithium for < 24 months; LE = patients with BP-I exposed to lithium for > 24 months; HC = healthy controls; df = degrees of freedom; PLSD = protected least significant difference; SD = standard deviation.

Table 3. Post-Hoc comparisons of amygdala and hippocampal volumes

Anatomical region	Side	*p* Fisher's PLSD contranst					
		NE vs HC	SE vs HC	LE vs HC	SE vs NE	LE vs NE	SE vs LE
Post-Hoc							
Amygdala	Right	**<0.001**	0.61	0.17	**0.002**	**0.021**	0.39
	Left	**<0.001**	0.58	0.15	**0.002**	**0.018**	0.99
Hippocampus	Right	**<0.001**	**0.001**	0.24	0.073	**0.016**	**0.03**
	Left	**<0.001**	**0.001**	0.15	0.99	**0.047**	**0.04**

ANOVAs were performed on total subcortical volumes corrected for intracranial volume (ICV). Significant p-values ($p < 0.05$) are indicated in bold. BP-I = Type I bipolar disorder; NE: patient with BP-I naïve to treatment with lithium; SE = patients with BP-I exposed to lithium for < 24 months; LE = patients with BP-I exposed to lithium for > 24 months; HC = healthy controls; PLSD = protected least significant difference.

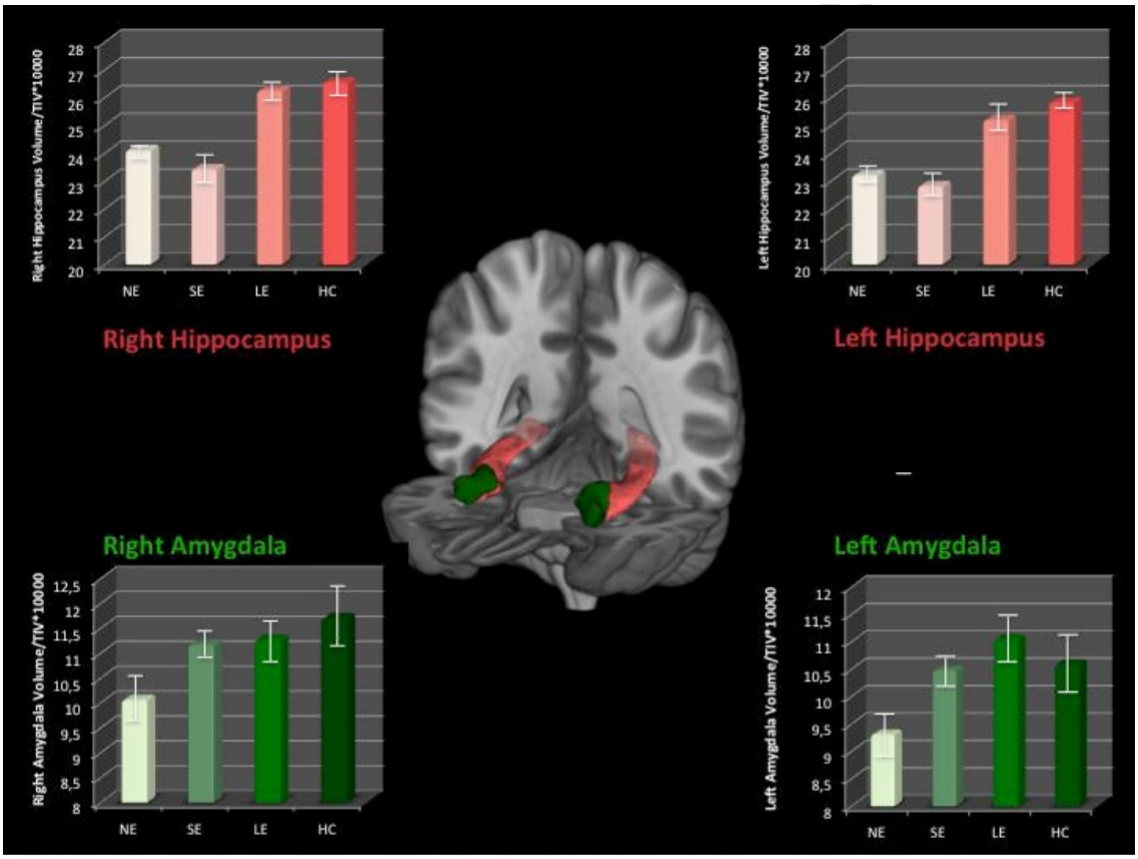

Fig. 1. Top: Mean volumes and standard errors of the right and left hippocampus in each subject group. Bottom: Mean volumes and standard errors of the right and left amygdala in each subject group. Center: 3D map of the hippocampus and the amygdala. BP-I: Type I bipolar disorder; NE = patients with BP-I never exposed to lithium; SE = patients with BP-I exposed to lithium for < 24 months; LE = patients with BP-I exposed to lithium for > 24 months; HC = healthy controls; TIV: total intracranial volume.

3.4 Discussion

The present study demonstrates that the effect of lithium treatment on limbic and subcortical volumes among persons with BD-I varies by duration of lithium exposure. NE BD-I had smaller bilateral hippocampal and amygdalar volumes than individuals without BD-I (i.e., HC). The volumes of these structures did not differ between persons with LE BD-I and either individuals without BD-I or individuals with BD-I who were lithium-treatment naïve.

Although limbic and subcortical volumes among individuals with BD-I who received long-term lithium treatment did not differ from HC, those with BD-I who received short-term lithium treatment demonstrated greater amygdalar volumes than those with BD-I who were lithium-treatment naïve. Individuals with BD-I who received short-term lithium treatment also demonstrated smaller bilateral hippocampal volumes than those with BD-I and either long-term lithium treatment patients or those without BD-I, and no differences from those with BD-I who were lithium-treatment naïve. These findings may reflect opposite effects of illness burden and lithium on the hippocampus and the amygdala.

Hippocampus and amygdala are part of two large scale, selective distributed neural networks involved in the emotion generation, expression, experience and control (Mega *et al.*, 1997). The amygdala is the subcortical focus

of a ventral limbic-paralimbic-subcortical-caudal network involved in emotional generation and expression (i.e., motor, endocrine, autonomic and visceral reactions to internal and external stimuli) while the hippocampus is a critical node in a dorsal limbic-paralimbic-neocortical network involved in subjective emotional experience, emotional regulation, and cognitive associations with emotion (Arciniegas *et al.*, 2013).

The pathophysiology of mood disorders mainly involves alterations in the cerebral networks' structure and/or function as well as their interactions (Arciniegas *et al.*, 2013; Phillips *et al.*, 2003). Consistent with this view of the pathophysiology of mood disorders, alterations in the structure and/or function of the hippocampus and amygdala are often described in associations with bipolar disorder (Phillips and Swartz, 2014). Post-mortem (Benes *et al.*, 1998; Bowley *et al.*, 2002) and clinical studies (Hajek, Cullis, *et al.*, 2012; Hartberg *et al.*, 2015) demonstrate lower numbers of neurons and smaller gray matter volumes among individuals with bipolar disorder who are lithium-treatment naïve.

Accordingly, the observation of essentially normal limbic volumes among persons with LE BD-I in the present study suggests a possible neuroprotective or neurorestorative effect of lithium against illness-related alterations in these structure (Germaná *et al.*, 2010; Hartberg *et al.*, 2015; Johnson *et al.*, 2009; Selek *et al.*,

2013; Wood *et al.*, 2004). The present findings also suggest that this putative neuroprotective or neurorestorative effect also may be conferred by short-term lithium treatment but that this effect, in this context, is limited to the amygdala. Treatment with lithium exerts an acute effect on amygdalar activation (Strakowski *et al.*, 2016) and is associated with preservation of amygdalar volumes (Selek *et al.*, 2013). These short-term effects of lithium on the amygdala may contribute to its acute mood stabilizing properties, which usually begin within a few weeks of treatment initiation (Malhi *et al.*, 2013). These acute effects are sustained overtime (Hartberg *et al.*, 2015; Usher *et al.*, 2010) and thereby protect the amygdala from damage induced by multiple mood episodes reflected in the smaller amygdalar volumes of patients with BD-I who are lithium-treatment naïve.

The present findings suggest that long-term treatment with lithium may have a beneficial effect on hippocampal volumes in BD-I, consistent with the beneficial effects of long-term (Yucel *et al.*, 2007), but not short-term (Kropf and Muller-Oerlinghausen, 1979), lithium treatment on memory. Indeed, short-term lithium treatment is associated with impairment in free recall memory (*ibidem*) whereas long-term lithium treatment improves recollection memory performances, in association with increased hippocampal volumes (Yucel *et al.*, 2007).

The mechanism by which lithium exerts its possible neuroprotective and/or neurorestorative effect(s) and the differential mechanisms that inform short versus long-term neuroprotective effects (or their absence) remain incompletely defined. Short-term lithium monotherapy is not associated with increased hippocampal levels of N-acetyl-aspartate (NAA), an indirect marker of neuroprotection (Zanetti *et al.*, 2015), whereas preserved levels of hippocampal NAA were found in patients with more than ten years of constant lithium assumption (Colla *et al.*, 2009). Clinical studies also demonstrated that long-term and constant lithium assumption is associated with reduced risk of developing Alzheimer's Disease (Blennow *et al.*, 2006), while short-or no-exposure to lithium is related to a higher risk (Colla *et al.*, 2009).

Consistent with the temporal differential of lithium treatment on amygdalar and hippocampal volumes observed in the present study, lithium-induced glutamate regulation occurs earlier in the amygdala than in the hippocampus (Gray and Mcewen, 2013; Higashitani *et al.*, 1990; Maruta *et al.*, 2005). In fact, chronic lithium administration reverses stress-related remodeling of dendritic arbors in both areas (Gray and Mcewen, 2013; Johnson *et al.*, 2009) via the downregulation of glutamatergic signaling, and acute intraperitoneal injection of lithium reduces calcium-dependent NO3 levels in the amygdala, acting on the same mechanism (Wood *et al.*, 2004). By contrast, short-term

treatment with lithium does not efficiently modulate glutamate-induced increase of calcium levels in the hippocampus (Maruta *et al.*, 2005). Moreover, amygdalar activation induces long-term modifications in the hippocampus during memory formation processes through glutamatergic signaling (Higashitani *et al.*, 1990), and the dysregulation of the glutamatergic transmission (Abe, 2001; Ikegaya *et al.*, 1995) induces hippocampal dysfunction (Roozendaal *et al.*, 2001).

Collectively, these observations suggest that the delayed action of lithium on the hippocampus may be mediated by its modulatory effects on glutamate signaling in the amygdala which, in turn, induces long-term modifications of hippocampal function and, ultimately, structure (reflected in the volume of this structure).

3.5 Limitations

The observations made in the present study and conclusions drawn from them are limited by its retrospective and cross-sectional design. A longitudinal study that includes protections against rater bias (i.e. masking of neuroimaging analyses) is needed to confirm the present observations of a possible neuroanatomical selective and time-dependent effect of lithium on limbic and subcortical volumes.

Furthermore, a neuropsychological evaluation in those patients is also needed to verify if differences in neurobiology are accompanied by differences in cognitive performances. The strength of any claims regarding the specificity of the effects observed as associated to duration of lithium treatment also must be tempered by acknowledgement of other concurrent treatments received by participants in this study, including anticonvulsants or atypical antipsychotics, many of which appear to have predominantly normalizing effects on brain structure in BD (Hafeman *et al.*, 2012). For this reason, chi-square tests were performed between BD groups and demonstrated no differences in the past and present pharmacological.

CHAPTER 4

Study 3: Lithium treatment impacts nucleus accumbens shape in bipolar disorder

4.1 Introduction

As highlighted also in chapter three, brain changes in deep grey matter (DGM) structures of patients with diagnosis of Bipolar Disorder (BD) (Hibar *et al.*, 2016) have been described previously but with some inconsistences (McDonald *et al.*, 2004). As mentioned in study two, the sources of these heterogeneity are multifactorial and one much debated source of bias is the effect of mood-stabilizing medications, primarily lithium (the archetypal mood stabilizer), in terms of volumetric increase induced on brain structures, particulary hippocampus and amygdala (De-Paula *et al.*, 2016; Manji *et al.*, 2000; Shaltiel *et al.*, 2007; Simonetti *et al.*, 2016).

In recent years, developments in brain morphometric methodologies have led to different structural measures that can integrate data derived from volumetric analysis. Indeed, investigation of the three-dimensional surfaces of DGM structures have been shown to be more sensitive than gross morphometric techniques, identifying group abnormalities

where volumetric analysis did not (Mamah *et al.*, 2009). Since shape analysis enables the uncovering of localized changes on the surface of brain structures, it can be a very specific neuroimaging technique, especially in the case of structures with explicit regional differentiation in functions, such as DGM (Herrero *et al.*, 2002). Previous studies investigating DGM shape in BD reported that drug-naive and non-psychotic BD patients, compared with healthy controls (HC), show widespread shape alteration of the caudate (Hwang *et al.*, 2006; Ong *et al.*, 2012) and putamen (Hwang *et al.*, 2006), both as local inward and outward deformations. Significant shape contraction on the ventral surface of the right accumbens and anterior expansion of the globus pallidus nuclei in non-psychotic BD patients have also been reported (Mamah *et al.*, 2016). However, results from these studies did not consider the specific effect of lithium treatment. Consequently, also the relationship between lithium-driven DGM shape variations and clinical correlates of BD patients, such as the degree of depressive and manic symptoms, was not investigated.

In the present work, our first aim was to analyse the potential effect of the duration of lithium treatment on the morphometric measures of DGM surface. As a secondary goal, we aimed at identifying the relationship between the severity of patients' depressive and/or manic symptomatology and the degree of any localized DGM abnormalities. To this aim we analysed the shape of seven

bilateral DGM structures (i.e. Accumbens, Amygdala, Caudate, Hippocampus, Pallidus, Putamen, and Thalamus) in BD (both as a whole group and stratified according to lithium treatment duration) and HC samples. We hypothesized (i) BD patients' DGM structures shape as modulated by lithium treatment duration, (ii) the DGM surface differences between BD and HC subjects as a function of lithium treatment duration and (ii) that such differences are associated to the severity of depressive and (hypo)manic patients' symptomatology.

4.2 Methods and Materials

Ethical permission was obtained from the local ethic committee of the Santa Lucia Foundation for this cross-sectional case-control study. All participants provided written informed consent to be included in the study. An a priori power calculation in G*power was used to determine the minimum sample size. Specifically, given the lack of prior studies about the relationship between DGM shape morphometry and lithium treatment, we used data from our prior studies on hippocampal volumetry in BD, which show effect sizes of 0.85-0.99 for lithium-dependent modulatory effects, to inform the power calculation. To be conservative we used the lower estimate in a power calculation using G*Power statistical software (Erdfelder *et al.*, 2009), which

determined that a total sample size of at least 24 subjects would have greater than 95% power to detect a difference between groups, with an alpha value of <0.05 (two tailed).

Participants

Eighty patients with a diagnosis of BD (48 BD type I – 32 BD type II) according to the Diagnostic and Statistical Manual of Mental Disorders IV-Edition, Text Revised (DSM-IV-TR) (American Psychiatric Association, 2000) were initially assessed at the Santa Lucia Foundation in Rome. As for study one and two, during diagnostic process the clinical psychiatrist who had been treating the patients and knew their clinical history, and who was blind to the aims of the study, made the preliminary diagnosis using the DSM-IV-TR criteria. Then, a research psychiatrist using the Structured Clinical Interview for DSM-IV-TR-Patient Edition (SCID-I/P) (M. B. First et al., 2002) confirmed the clinical diagnoses. If the diagnoses made at the two different steps were not consistent, more data were gathered and the diagnostic process continued until a final diagnostic consensus was reached. If an agreement could not be reached, the patient was removed from the sample.

Inclusion criteria for all participants were: (i) age between 18 and 75 years, (ii) at least five years of education, and (iii) suitability for magnetic resonance imaging (MRI)

scanning. Exclusion criteria were: (i) history of alcohol or drug abuse in the two years before the assessment, (ii) lifetime drug dependence, (iii) traumatic head injury with loss of consciousness, (iv) past or present major medical illness or neurological disorders, (v) any (for HC) or additional (for patients with BD) psychiatric disorder or mental retardation, (vi) dementia or cognitive deterioration according to DSM-IV-TR criteria, and Mini-Mental State Examination (MMSE) (Folstein *et al*., 1975) score <25, consistent with normative data in the Italian population (Measso *et al*., 1993), (vii) low quality of T1- weighted images (i.e. presents of severe motion or scanner-generated artefacts), (viii) any potential brain abnormality or microvascular lesion as apparent on conventional fluid attenuated inversion recovery (FLAIR) scans, potentially explaining critical phenomenology; in particular, the presence, severity, and location of vascular lesions were computed according to the semi-auto- mated method recently published by our group (Iorio *et al.*, 2013).

From the original BD group (n=80), two refused to undergo the MRI exam and four were excluded for the low quality of T1- weighted images (see exclusion criteria). The remaining sample of 74 patients included 45 with BD-I and 29 with BD-II.

We also recruited 74 healthy controls (HC) in the same geographical area, paired-matched with the patients for age, gender and educational level. All HC were screened for a

current or lifetime history of DSM-IV-TR Axis I and II disorders using the Structured Clinical Interview for DSM-IV-TR Axis I Disorders, Research Version, Non-patient Edition (SCID-I-NP) (M. B. First *et al.*, 1997) and Structured Clinical Interview for DSM-IV Axis II Personality Disorders (SCID-II) (M. First *et al.*, 1997); they were also assessed to confirm that no first-degree relative had a history of bipolar, mood- or schizophrenia-related disorders.

Clinical Assessment

All patients were under stable pharmacologic treatment for at least six months, usually polypharmacy, including treatment with lithium, antidepressants, other mood-stabilizing agents, and stable oral dosages of one or more antipsychotics (data not shown; available upon request). For patients treated with lithium, we also collected specific information about treatment duration (LiTD), reported in months. Age at onset was defined as 'age at onset of first affective symptoms', which were investigated in an interview with patients and first-degree relatives. Moreover, we categorized patients with LiTD higher than 50% of illness duration (hereafter called LiTD+, N=13), those with LiTD shorter than 50% of illness duration (LiTD-, N=31), and those not taking lithium at all (NoLi, N=30), in order to weight up LiTD as a function of patients' illness duration.

This was done in order to obtain better homogeneity (in terms of drug exposure) of samples.

The overall severity of affective depressive and (hypo)manic symptoms was assessed using the 17-item Hamilton Depression Rating Scale (HAM-D) (Hamilton, 1960), the Beck Hopelessness Scale (BHS) (Beck, 1998) and the Young Mania Rating Scale (YMRS) (Young *et al.*, 1978). The amount of depressive symptoms were scored rating also the psychological and somatic components of depression, apart from the final account (i.e. HAM-D_{tot}, HAM-D_{psy}, HAM-D_{som}).

Image acquisition e processing

All 148 participants underwent the same imaging protocol, which included 3D T1-weighted, T2- weighted and FLAIR sequences using a 3T Achieva MR scanner (Philips Medical Systems, Best, The Netherlands) with a 32-channel receiving-only head coil. Whole-brain T1- weighted images were obtained using a fast-field echo sequence (echo time/repetition: time = 5.3/11 msec, flip angle = 9°, voxel size = 1×1×1 mm3). T2 and FLAIR sequences were acquired to screen for brain pathology.

Segmentations of seven bilateral subcortical grey matter nuclei (accumbens, amygdala, caudate, hippocampus, globus pallidus, putamen and thalamus) were generated

using the FIRST algorithms included in the FMRIB Software Library (FSL, version 5.0.0) and are fully described in the Appendix (see Appendix). After the automated segmentation by the software, the outputs were manually checked and confirmed for the proper nuclei extraction of all the subcortical structures. FSLView toolbox was used for neuroimaging results visualizations (http://fsl.fmrib.ox.ac.uk/fsl/fslwiki/FslView).

In case of significant results located in the nucleus accumbens, we further refined their localization in terms of specific accumbens subregions (i.e. core and shell), by using the Human Brain Atlas and referring to previous evidence on accumbens anatomy (Baliki *et al.*, 2013).

Statistical Analyses

Comparisons between HC and BD on sociodemographic (i.e. age, gender, and educational level) and between BD subgroups on clinical (i.e. duration of illness, number of episodes, time of lithium exposure, severity of (hypo)manic/depressive symptoms and pharmacological treatment) characteristics were performed using t-test, ANOVA or chi-square tests on StatView statistical software, considering $p < 0.05$ as statistical significances.

All neuroimaging statistics were performed by vertex-wise shape analysis along the surface of the segmented

subcortical structures, using FSL Randomise tool with a nonparametric permutation testing (Nichols and Holmes, 2002). We used n=5000 permutation and a Threshold-Free Cluster Enhancement (TFCE, --T2) to correct for multiple comparisons ($p < 0.05$, after correction for multiple comparisons) (Smith and Nichols, 2009).

We preliminary checked for the presence of DGM morphological differences between BD-I and BD-II performing t-tests between patients' subgroups. Since no difference was found between BD subtypes, t-test comparisons for the same areas were performed between BD and HC, considering BD patient group as a whole.

The assessment of the effect of lithium treatment duration on BD DGM was investigated as follows: first, linear regressions were performed between each DGM shape measure of BD (continuous dependent variable) and LiTD (continuous independent variable), including the duration of illness as covariate of no interest. The inclusion of the covariate was justified by the presence of an association with the independent variable ($r= 0.354$, $p= 0.0186$). Second, in case of significant linear regressions results, comparison between HC and BD were performed categorizing BD patients in groups according to LiTD. To this aim, ANOVA analyses were conducted for each DGM where significant correlations results were found, using shape as dependent variable and group (i.e. LiTD+, LiTD-, NoLi, HC groups) as four-level independent variable. In

case of ANOVA results surviving the $p<0.05$ corrected threshold, post-hoc t-tests were performed.

The relationship between significant BD shape alterations (independent variable) and clinical symptoms severity (i.e. HAM-D_{tot}, HAM-D_{psy}, HAM-D_{som}, BHS_{tot}) (dependent variable) was assessed performing linear regressions. Nuclei surface areas resulted in significant outward or inward deformations from the ANOVA comparisons were used as binary region of interest (ROI masks) to restrict subsequent post-hoc and linear regressions analyses.

4.3 Results

Sociodemographic and clinical characteristics

Sociodemographic characteristics of BD and HC groups as well as clinical variable of NoLi, LiTD- and LiTD+ are shown in Table 1. BD (total sample and sub-groups) and HC were not different for age, gender or educational level (Table 1). Apart from lithium treatment, the patient groups did not differ significantly in terms of duration of illness, number of mood episodes and pharmacological treatment (Table 1).

Table 1. Sociodemographic and clinical characteristics of 74 BD patient and, 74 healthy subjects. Bottom section refers to the BD lithium treatment duration-based patients stratification: 31 BD_LiTD-; 13 BD_LiTD+; 30 BD_NoLi.

Characteristics	BD	HC	t, F or χ2	df	p
Age (years), mean (SD)	43.96 (12.4)	43.96 (17.2)	0.00	146	-
Males, n (%)	42 (56.8)	42 (56.8)	0.00	1	-
Educational level (years), mean (SD)	14.2 (3.3)	14.8 (2.9)	-1.221	146	0.224
Duration of illness (years), mean (SD)	14.9 (10.7)	-	-	-	-
Number of past manic/hypomanic episodes, mean (SD)	5 (6.2)	-	-	-	-
Number of past depressive episodes, mean (SD)	6.2 (6.4)	-	-	-	-
HAM-D score, mean (SD)	7.7 (5.6)	-	-	-	-
YMRS score, mean (SD)	5 (6)	-	-	-	-
Current medication, n (%)	74 (100)	-	-	-	-
Antidepressant, n (%)	29 (39.2)	-	-	-	-
Antipsychotics, n (%)	47 (63.5)	-	-	-	-
Lithium, n (%)	44 (59.5)	-	-	-	-
Benzodiazepines, n (%)	29 (39.2)	-	-	-	-
Other treatments	-	-	-	-	-

Characteristics	BD_LiTD-	BD_LiTD+	BD_NoLi	HC	t, F or χ2	df	*p*
Age (years), mean (SD)	44.7 (13)	45 (11)	42.7 (12)	43.9 (17)	0.112	3	0.952
Males n (%)	22 (71)	6 (46.2)	14 (46.7)	42 (57)	4.391	3	0.1113
Educational level (years), mean (SD)	14.7 (3.5)	14.3 (3)	13.6 (3.1)	14.8 (2.8)	1.199	3	0.312
Duration of illness (years), mean (SD)	17.2 (10.5)	11.5 (9.1)	14.3 (11.3)	-	0.21	71	0.319
Duration of lithium treatment (months), mean (SD)	41.4 (34)	91.8 (63.3)	-	-	-3.4	42	0.0013*
Number of past manic/hypomanic episodes, mean (SD)	4.1 (3)	4.2 (3.1)	6.31 (9)	-	1.12	2	0.336
Number of past depressive episodes, mean (SD)	5.4 (4)	5.9 (4)	7 (8.9)	-	0.459	2	0.633
HAM-D score, mean (SD)	7.2 (6.6)	6.8 (5.6)	8.5 (4.4)	-	0.586	2	0.559
YMRS score, mean (SD)	3.2 (4.3)	6.7 (5.5)	6.2 (7.3)	-	2.69	2	0.075
Antidepressant, n (%)	10 (32.3)	3 (23.1)	16 (53.3)	-	4.559	2	0.102
Antipsychotics, n (%)	20 (64.5)	8 (61.5)	19 (63,3)	-	0.036	2	0.982
Benzodiazepines, n (%)	13 (41.9)	4 (30.8)	12 (40)	-	0.493	2	0.781
Other treatments							

Shape Analysis

Both comparisons between BD-I and BD-II patients and between HC and BD (considered as a single diagnostic group) did not show significant differences in any of the DGM structures.

When evaluating the linear relationship between LiTD and DGM shape in BD, we found significant correlations in right and left accumbens nuclei (R-Accu and L-Accu, respectively). As stated above, in order to qualify the localization of significant deformation in terms of specific accumbens subregions (i.e. core or shell), we both referred results to the standard Human Brain Atlas (available at http://human.brain-map.org/) and to previous evidence for human nucleus accumbens anatomy(Baliki *et al.*, 2013). As for the latter, we employed the MNI coordinates previously reported(Baliki *et al.*, 2013) who anatomically defined the core and the shell of the nucleus accumbens. Coordinates were thus used as reference to create regions of interest corresponding to core or shell where our results were superimposed on. According to y-axis coordinate(Baliki *et al.*, 2013) and to boundaries obtained from *Human Brain Atlas,* our results can be selectively located on the surfaces of the accumbens nuclei core or shell. Specifically, we found positive correlations bilaterally in clusters within the accumbens core sub-field (statistical peaks: corrected $p_{R\text{-}Accu\text{-}Core} = 0.016$; corrected $p_{L\text{-}Accu\text{-}Core} = 0.031$) indicating that the longer LiTD, the more outward is the bending of the cluster on the core (i.e. core extroflexion). Moreover, we found a negative correlation between shape and LiTD in a cluster on the boundary of the R-Accu shell sub-field (statistical peak: corrected $p_{R\text{-}Accu\text{-}Shell} = 0.002$), indicating

that LiTD is associated with inward bending in this region (i.e. shell introflexion) (Figure 1).

ANOVA performed on R-Accu and L-Accu shape between diagnostic groups (LiTD+, LiTD-, NoLi and HC) showed significant bilateral results (statistical peaks: corrected $p_{L\text{-}Accu\text{-}ANOVA}$=0.025; correced $p_{R\text{-}Accu\text{-}ANOVA}$=0.025) (Figure 2). Post-hoc t-tests revealed R-Accu shell outward deformation in the NoLi group compared to LiTD+ (statistical peak: corrected $p_{R\text{-}Accu\text{-}Shell}$ = 0.016) and HC (statistical peak: corrected $p_{R\text{-}Accu\text{-}Shell}$ = 0.002). Moreover, the LiTD- group showed L-Accu core inward deformation compared to HC (statistical peak: corrected $p_{L\text{-}Accu\text{-}Core}$ = 0.027). Details on results and clusters coordinates are shown in Table 2.

The shape of BD L-Accu-Core was positively correlated with HAM-D_{tot} score (statistical peaks: corrected $p_{L\text{-}Accu\text{-}core}$= =0.02), HAM-$D_{som}$ (statistical peaks: corrected $p_{L\text{-}Accu\text{-}core}$=0.005) and BHS_{tot} score (statistical peaks: corrected $p_{L\text{-}Accu\text{-}core}$=0.03) (Table 2, Figure 3), indicating the more inward deformation the higher depression symptom severity. No significant associations were found for $YMRS_{tot}$ scores.

Figure 1. **Relationship between patients' lithium treatment duration and nucleus accumbens shape morphometry**.
Linear regression results using lithium treatment duration (months) and accumbens nuclei shape deformations (distance from mean template, mm^3) as variables of interest. *a)* right accumbens shell; *b)* right accumbens core and *c)* left accumbens core; *d)* Statistical maps for significant (TFCE-corrected) right/left accumbens core inward and right accumbens shell outward deformations (in red) superimposed onto representative nucleus accumbens masks (light blu). Borders of shell and core nuclei are drawn using solid black lines and taken from the *Human Brain Atlas* (available in http://human.brain-map.org/).

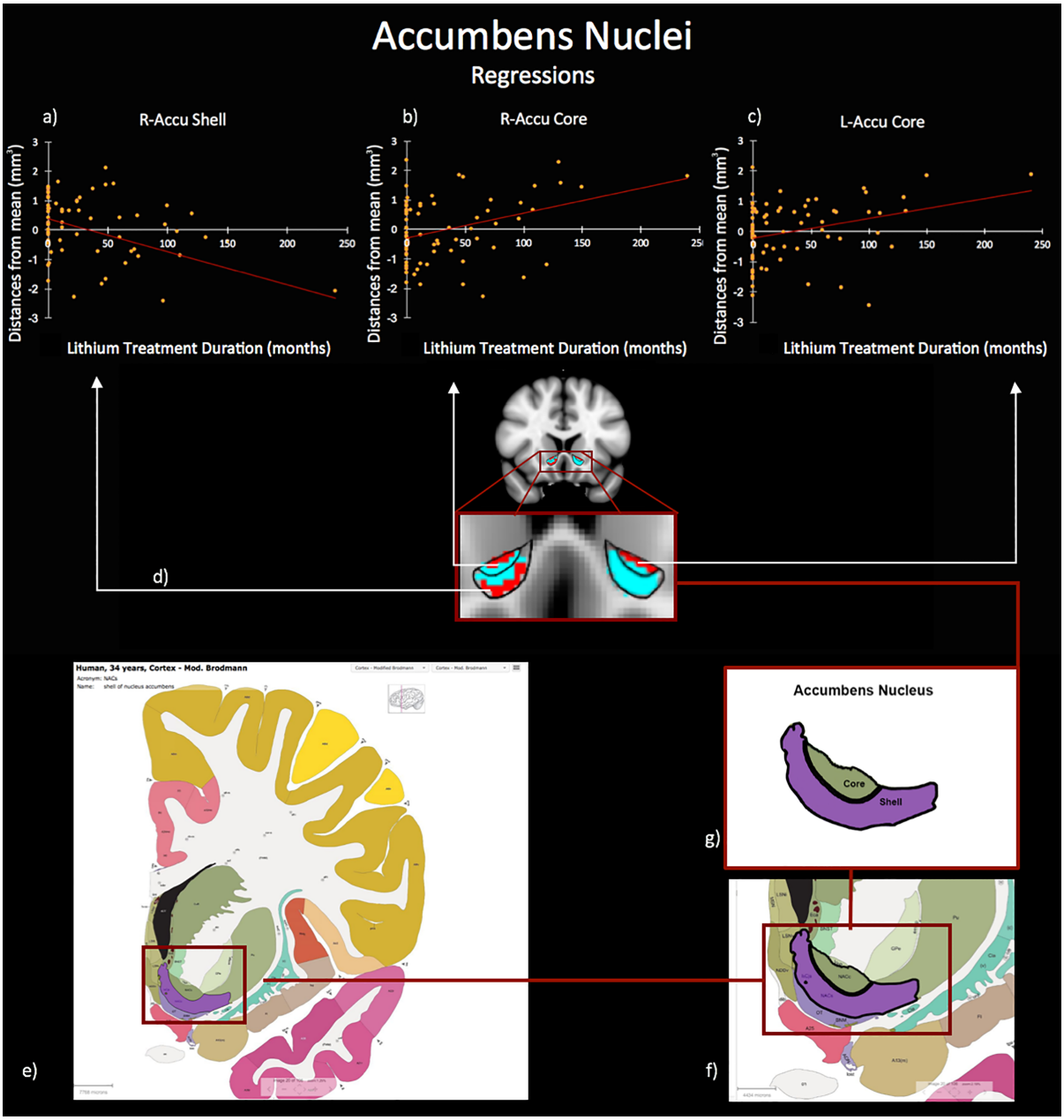

***Figure 2*. Comparison between healthy subjects and patients with bipolar disorder stratified according to lithium treatment duration.**
a) 3D visualization of ANOVA results: right accumbens shell outward and left accumbens core inward deformations (in red) superimposed onto a representative nucleus accumbens mask (in blue); *b)* Mean total deformation (distance from mean template, mm^3) of right accumbens shell (grey) and left accumbens core (orange) in patients with lithium treatment duration longer/shorter then 50% of illness duration (respectively, BD_LiTD+, BD_LiTD-), patients never treated with lithium (BD_NoLi)

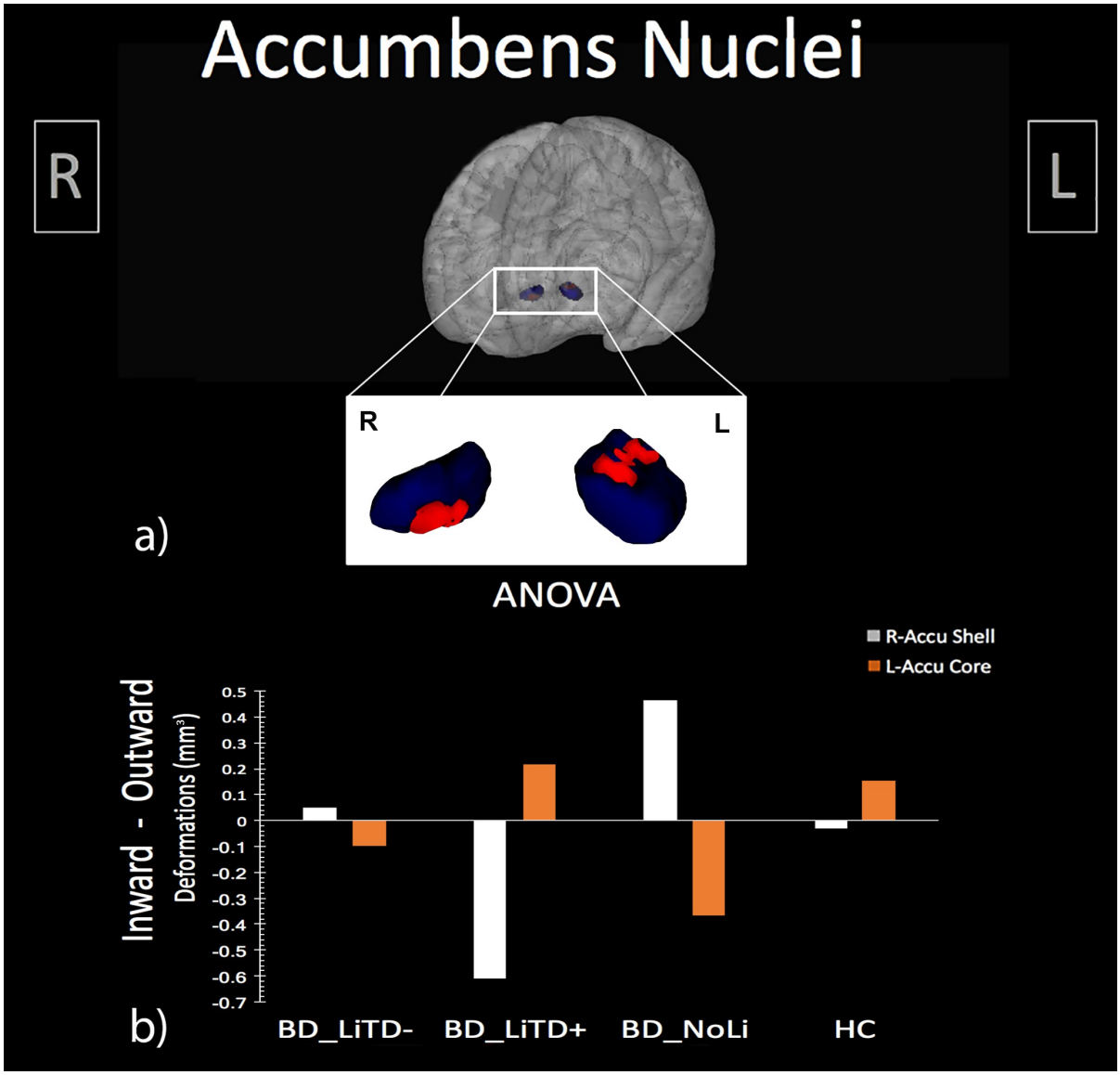

Figure 3. **Clinical correlates of left accumbens inward deformation.** Relationship between deformations resulted from ROI ANOVA and patients depressive/hopelessness symptom scores, assessed through a) Somatic subscale of Hamilton Depression Rating Scale (HAM-Dsom); b) Total score of Hamilton Depression Rating Scale (HAM-Dtot); c) Total score of Beck Hopelessness Scale (BHStot).

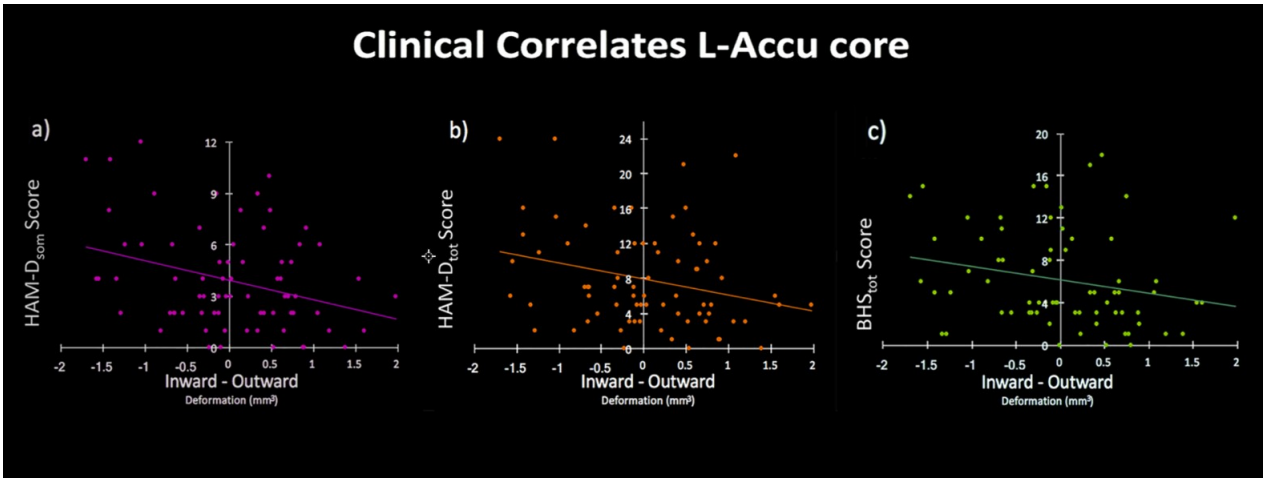

Table 2. Neuroimaging Results. Topography of significant relationships between BD LiTD and boundary deformation on the left/right accumbens nuclei shape morphometric feature. Effects have been assessed through linear regression analyses, ANOVA comparisons between BD groups stratified according to LiTD (i.e. BD_LiTD-, BD_LiTD+, BD_NoLi) and HC and related post-hoc analyses. Clinical correlates (depressive/hopefulness BD symptoms scores) of L-Accu core inward deformation are also reported.

Anatomical region	Results	Cluster Exent (mm3)	R^2/F/t	statistical peak *p* (TFCE-corrected)	MNI Coordinates of the statistical peak		
					x	y	z
Regression Analyses							
Left Nucleus Accumbens core	Positive Correlation	68	0.1	0.031*	-0.15	19	-6
Right Nucleus Accumbens core	Positive Correlation	56	0.12	0.016*	10	14	-4
Right Nucleus Accumbens shell	Negative Correlation	136	0.17	0.002*	8	13	-10
ANOVA							
Left Nucleus Accumbens core		47	F(3;144)= 4.59	0.01	-11	16	-4
Right Nucleus Accumbens shell		55	F(3;144)= 3.5	0.025	8	13	-9
Post-Hoc							
Left Nucleus Accumbens core	BP_LiTD- < HC	17	2.72	0.027*	-10	16	-9
Left Nucleus Accumbens core	BP_NoLi < HC	47	3.5	0.002*	-10	16	-9
Left Nucleus Accumbens core	BP_NoLi < BP_LiTD+	47	2.32	0.016*	-10	9	-6
Right Nucleus Accumbens shell	BP_NoLi > BP_LiTD+	55	3.11	0.005*	8	14	-10
Right Nucleus Accumbens shell	BP_NoLi > HC	55	2.58	0.005*	10	18	-9
Clinical Correlates							
HAM-Dsom	Positive Correlation	43	0.1	0.005*	-12	10	-6
HAM-Dtot	Positive Correlation	41	0.07	0.02*	-12	9	-6
BHStot	Positive Correlation	18	0.05	0.03*	-9	16	-3

TFCE, Threshold-Free Cluster Enhancement; Coordinates are in Montreal Neurological Institute Space. BD_LiTD-, bipolar disorder patients with lithium duration treatment shorter then 50% of illness duration; BD_LiTD+, bipolar disorder patients with lithium duration treatment longer then 50% of illness duration; BD_NoLi, bipolar disorder patients never treated with lithium; HC, healthy control subjects. HAM-Dsom, somatic subscale from Hamilton Depression Rating Scale; HAM-Dtot score from Hamilton Depression Rating Scale; BHStot, total score from Beck Hopefulness Scale.
**Statistically significant differences at $p < 0.05$.*

4.4 Discussion

Effects of lithium treatment duration on DGM shape is relevant in BD patients and possible deformations are linked to the depressive and (hypo)manic phenomenology. Indeed, we found significant bilateral extroflexction effect dependent to increased duration of lithium treatment on the core of BD accumbens surfaces, while a concomitant introflection effect was found on the shell of right

accumbens. A further analysis between groups with different treatment duration, showed that NoLi e LiTD- groups had inward/outward deformations both on L-Accu core and R-Accu shell surfaces when compared to HC and LiTD+. L-Accu core boundary inward deformation was also found comparing LiTD- group and HC. We also found that only deformation of L-Accu-Core shape was significantly correlated with increased depression severity.

To the best of our knowledge, this is the first report describing an association between lithium treatment duration and accumbens nuclei shape in BD patients. Previous studies investigating the impact of lithium treatment on brain structures, mainly focused on volume (Hibar *et al.*, 2016; Alessio Simonetti *et al.*, 2016) and cortical thickness (Giakoumatos *et al.*, 2015). Results revealed a trophic effect of lithium treatment resulting in volume preservation of deep grey matter assemblies (e.g. hippocampus, amygdala, thalamus and basal ganglia) and cortical thickening in frontal, parietal and occipital regions as well as in the precuneus and precentral areas (Abramovic *et al.*, 2016; A. Simonetti *et al.*, 2016). This was also confirmed by post-mortem studies demonstrating lower numbers of neurons among individuals with BD who are lithium-treatment naïve (Benes *et al.*, 1998; Bowley *et al.*, 2002). As for the nucleus accumbens, animal studies found that lithium modulates neuronal activity and neurotransmission in models of the disorder. In particular,

chronic administration of lithium reverses many of the phenotypes of *Clock-Δ19* mice, which display behaviours (i.e. increased exploratory drive in novel environments, significant reduction in sleep, decreased anxiety related behaviours, and increase in cocaine preference) that are very similar to those found in the manic phase of human BD. Interestingly, Clock-Δ19 mice have higher dopamine levels in the nucleus accumbens and chronic lithium treatment decreases dopamine tissue levels in their nucleus accumbens (Coque *et al.*, 2011). Along this line of evidence, it has been shown that chronic lithium treatment regiment inhibits dopamine neurotransmission in the nucleus accumbens (Can *et al.*, 2016). However, acute lithium treatment did not elicit the same reduction in dopamine amplitude following 60 Hz pulse train stimulation in the ventral tegmental area, suggesting that long-term lithium administration ameliorates mania phenotypes by stabilizing the readily releasable dopamine pool in ventral tegmental area axon terminals in the nucleus accumbens. However, direct evidence of potential effects of lithium treatment duration on nucleus accumbens morphometry in humans is still lacking.

The nucleus accumbens is connected to the limbic and extrapyramidal motor systems and, having dopamine as a principal neurotransmitter, has a central role in the cerebral reward system. Acting as a limbic-motor interface, it regulates motivation and emotional processes and is involved in the mechanisms of a number of the most

disabling neuropsychiatric disorders (Mavridis *et al.*, 2011). Moreover, together with the cingulate cortex, the nucleus accumbens is a component of the anatomically defined basal ganglia–thalamocortical circuit (Alexander *et al.*, 1990; Devinsky *et al.*, 1995), that is considered to be a key element of the functional organization of the limbic system, and is often implicated in mood regulation (Groenewegen *et al.*, 1996). Owing in part to its neuroanatomical connectivity, the nucleus accumbens has been proposed to integrate mnemonic and emotional signals within the limbic system, linking nodes in the frontal and temporal lobes and determining the response priorities of an organism. Thus, the nucleus accumbens is thought to integrate these signals and turn them into action, via output to pallidal and other subcortical motor effector sites through which signal outflow from this region may bias the direction and intensity of behaviour. Recently, Has been proposed a more accurate way for characterizing its functions, overcoming the pedantic view that the nucleus accumbens merely acts as a reward centre relay (Floresco, 2015). Specifically, the nucleus accumbens is involved in modulation of cerebral processing of motivationally relevant goals by promoting likelihood, efficiency, and vigour of behaviours intended to obtain those goals, driving exploration of novel stimuli and procurement of things worth having (rewards) or the avoidance of aversive consequences. Moreover, the core and shell areas modulate different functions in this motivational

process: the core has a more prominent role in instigating approach behaviour toward motivationally relevant stimuli ("*go to it*" function) while the shell drives behaviour to stay on tasks until the rich of a goal ("*stay to it*" function), suppressing irrelevant or non-rewarded actions.

Evidence for reward and dopamine neural systems alterations in mood disorders like mania, major depression and BD have been widely reported both in humans and animal models (Abler *et al.*, 2008; Naranjo *et al.*, 2001; Nestler and Carlezon, 2006; Satterthwaite *et al.*, 2015). Furthermore, it has been proposed a "dopamine dysregulation syndrome" model for the BD pathophysiology (Berk *et al.*, 2007), where a cyclical dysregulation in quantitative dopaminergic transmission is the main construct. Even if our work does not directly asses this aspect related to dopamine release, our results support this model, showing a complex pattern of lithium-dependent surface modulatory effects on such central node for dopamine and rewarding systems.

The second important result of the present study is the association between left accumbens core inward deformation and both hopelessness and depressive symptom severity in areas of the core. Our results of the increased left core inward deformation associated with higher symptom severity support the hypothesis of a decreasing "go to it" brain signalling as pathophysiological correlate of depressive phenomenology in BD. Amotivational/anhedonic

features are crucial components of depression and, interestingly, the left lateralized finding of nucleus accumbens core deformation in BD may be explained by the crucial role of the dominant hemisphere in motivational behaviours (Pizzagalli *et al.*, 2005). Studies conducted over several decades support the use of long-term lithium treatment to prevent depression relapse in patients with bipolar disorder (Geddes *et al.*, 2004). In this context, our findings may reflect one of the neurobiological mechanisms underpinning the therapeutic effect of lithium, as part of its efficacy on preventing depression may unfold through a long-term remodeling of cortical-subcortical connections related to the motivational/hedonic dimension.

4.5 Limitations

Several issues have to be considered before concluding. First, the sample size of LiTD+ group is relatively small. However, it is adequate to detect shape differences because of the moderate to large effect size we observed. Second, our results should be replicated also with a longitudinal approach for definitively demonstrating a causal effect between lithium exposure and accumbens nuclei neuroprotection. Third, our patients were treated also with different psychotrophic drugs that might potentially affect accumbens nuclei shape. However, the BD subgroups

showed no differences in terms of non-lithium pharmacological drugs, making unlikely the probability that they may have influenced our results.

CHAPTER 5

Conclusions

Results from study 1, despite the above-mentioned limitations, are important for several reasons. Using a model based on cross-sectional case–control comparisons at different ages, the study demonstrated that the volumes of several brain areas are reduced from the very beginning of the illness course of BD, and that neurodegenerative features are not present. Moreover, we found that the brain areas showing volume reduction (the posterior cingulate cortex, cerebellum, thalamus, and posterior limb of the internal capsule) are strictly involved in mood and motor control processes. Since these reductions are present from the very beginning of the illness course, a role for these brain areas in the mechanism of BD is hypothesized. Lastly, our findings do not support the current distinction between the two types of BD based on the presence of mania or hypomania and suggest that patients with BD may belong to a unitary illness type, at least according to the data obtained here.

In study two, results about the effect of lithium exposure on limbic and subcortical gray matter volumes in BD-I appears to be time-dependent and relatively specific to the hippocampus and the amygdala, with short-term effects on the amygdala and long-term effects on both structures.

Finally, study 3 results are the first to demonstrate that duration of lithium treatment affects nucleus accumbens surface morphology in BD. Indeed, DGM morphometry in BD patients never treated with lithium compared to LiTD+ and HC group result in subtle shape abnormalities on bilateral accumbens nuclei surfaces, that is L-Accu core inward and R-Accu shell outward deformations. Coherently, we found that LiTD exerts a double significant morphometry effect, that is the core extroflextion and the shell introflextion, as the time of treatment increases. Morphometric features of L-Accu core surface deformation in BD group showed significant correlations with the severity of depressive phenomenology, being the less inward deformation associated to the lower depressions symptoms, especially in terms of somatic and components.

Taken together our results suggest that the duration of lithium treatment could act modulating and counteracting the BD accumbens microstructural baseline conditions as part of the mechanism of action in its mood stabilizing effects.

Results from studies 2 and 3 give strength to the clinical importance of long-term lithium treatment in BD-I. However, longitudinal prospective studies are necessary to confirm that the observed findings really reflect the effects of duration of lithium treatment on limbic and subcortical volumes and shape in BD-I.

References

A.H. Y. Lithium in maintenance therapy for bipolar disorder. J. Psychopharmacol. 2006; 20: 17–22.

Abe K. Modulation of hippocampal long-term potentiation by the amygdala: a synaptic mechanism linking emotion and memory. Jpn. J. Pharmacol. 2001; 86: 18–22.

Abler B, Greenhouse I, Ongur D, Walter H, Heckers S. Abnormal reward system activation in mania. Neuropsychopharmacology 2008; 33: 2217–27.

Abramovic L, Boks MPM, Vreeker A, Bouter DC, Kruiper C, Verkooijen S, et al. The association of antipsychotic medication and lithium with brain measures in patients with bipolar disorder. Eur. Neuropsychopharmacol. 2016; 26: 1741–1751.

Adler CM, DelBello MP, Jarvis K, Levine A, Adams J, Strakowski SM. Voxel-Based Study of Structural Changes in First-Episode Patients with Bipolar Disorder. Biol. Psychiatry 2007; 61: 776–781.

Alexander AL, Lee JE, Lazar M, Field AS. Diffusion tensor imaging of the brain. Neurotherapeutics 2007; 4: 316–29.

Alexander GE, Crutcher MD, DeLong MR. Basal ganglia-thalamocortical circuits: parallel substrates for motor, oculomotor, 'prefrontal' and 'limbic' functions. Prog. Brain Res. 1990; 85: 119–146.

Almeida JRC, Akkal D, Hassel S, Travis MJ, Banihashemi L, Kerr N, et al. Reduced gray matter volume in ventral prefrontal cortex but not amygdala in bipolar disorder: Significant effects of gender and trait anxiety. Psychiatry Res. - Neuroimaging 2009; 171: 54–68.

Altshuler LL, Bartzokis G, Grieder T, Curran J, Mintz J. Amygdala enlargement in bipolar disorder and hippocampal reduction in schizophrenia: An MRI study demonstrating neuroanatomic specificity [1]. Arch. Gen. Psychiatry 1998; 55: 663–664.

Altshuler LL, Curran JG, Hauser P, Mintz J, Denicoff K, Post R. T2 hyperintensities in bipolar disorder: magnetic resonance imaging comparison and literature meta-analysis. Am. J. Psychiatry 1995; 152: 1139–1144.

American Psychiatric Association. Diagnostic and Statistical Manual of Mental Disorders 4th revised edition. DSM-IV-TR. 2000.

American Psychiatric Association. DSM-5 Task Force. DSM 5. 2013.

Arciniegas DB, Wortzel HS, Frey KL. Behavioral Neurology & Neuropsychiatry. 2013.

Arnone D, Cavanagh J, Gerber D, Lawrie SM, Ebmeier KP, McIntosh a. M. Magnetic resonance imaging studies in bipolar disorder and schizophrenia: Meta-analysis. Br. J. Psychiatry 2009; 195: 194–201.

Ashburner J. A fast diffeomorphic image registration algorithm. Neuroimage

2007; 38: 95–113.
Ashburner J, Friston KJ. Unified segmentation. Neuroimage 2005; 26: 839–851.
Atmaca M, Ozdemir H, Cetinkaya S, Parmaksiz S, Belli H, Kursad Poyraz A, et al. Cingulate gyrus volumetry in drug free bipolar patients and patients treated with valproate or valproate and quetiapine. J. Psychiatr. Res. 2007; 41: 821–827.
Baldessarini RJ, Tondo L, Baethge CJ, Lepri B, Bratti IM. Effects of treatment latency on response to maintenance treatment in manic-depressive disorders. Bipolar Disord. 2007; 9: 386–393.
Baliki MN, Mansour A, Baria AT, Huang L, Berger SE, Fields HL, et al. Parceling Human Accumbens into Putative Core and Shell Dissociates Encoding of Values for Reward and Pain. J. Neurosci. 2013; 33: 16383–16393.
Bammer R. Basic principles of diffusion-weighted imaging. Eur. J. Radiol. 2003; 45: 169–184.
Bearden CE, Thompson PM, Dutton RA, Frey BN, Peluso MAM, Nicoletti M, et al. Three-dimensional mapping of hippocampal anatomy in unmedicated and lithium-treated patients with bipolar disorder. Neuropsychopharmacology 2008; 33: 1229–1238.
Beck AT. Beck Hopelessness Scale. J. Clin. Psychol. 1998; 54: 1063–1078.
Behrens TEJ, Johansen-Berg H, Woolrich MW, Smith SM, Wheeler-Kingshott CAM, Boulby PA, et al. Non-invasive mapping of connections between human thalamus and cortex using diffusion imaging. Nat. Neurosci. 2003; 6: 750–757.
Belmaker RH. Bipolar disorder. N. Engl. J. Med. 2004; 351: 476–486.
Benes FM, Kwok EW, Vincent SL, Todtenkopf MS. A reduction of nonpyramidal cells in sector CA2 of schizophrenics and manic depressives. Biol. Psychiatry 1998; 44: 88–97.
Berk KN. Tolerance and condition in regression computations. J. Am. Stat. Assoc. 1977; 72: 863–866.
Berk M, Dodd S, Kauer-Sant'Anna M, Malhi GS, Bourin M, Kapczinski F, et al. Dopamine dysregulation syndrome: Implications for a dopamine hypothesis of bipolar disorder. Acta Psychiatr. Scand. 2007; 116: 41–49.
Berman MG, Peltier S, Nee DE, Kross E, Deldin PJ, Jonides J. Depression, rumination and the default network. Soc. Cogn. Affect. Neurosci. 2011; 6: 548–555.
Blennow K, Leon MJ De, Zetterberg H. Seminar Alzheimer ' s disease. Lancet 2006; 368: 387–404.
Bluhm R, Williamson P, Lanius R, Théberge J, Densmore M, Bartha R, et al. Resting state default-mode network connectivity in early depression using a seed region-of-interest analysis: Decreased connectivity with caudate nucleus. Psychiatry Clin. Neurosci. 2009; 63: 754–761.
Bora E, Vahip S, Akdeniz F, Gonul AS, Eryavuz A, Ogut M, et al. The effect of previous psychotic mood episodes on cognitive impairment in euthymic bipolar patients. Bipolar Disord. 2007; 9: 468–477.
Bowley MP, Drevets WC, Öngür D, Price JL. Low glial numbers in the amygdala in major depressive disorder. Biol. Psychiatry 2002; 52: 404–412.

Brambilla P, Harenski K, Nicoletti MA, Mallinger AG, Frank E, Kupfer DJ, et al. Anatomical MRI study of basal ganglia in bipolar disorder patients. Psychiatry Res. - Neuroimaging 2001; 106: 65–80.
Breeze JL, Hesdorffer DC, Hong X, Frazier JA, Renshaw PF. Clinical Significance of Brain White Matter Hyperintensities in Young Adults with Psychiatric Illness. In: Harvard Review of Psychiatry. 2003. p. 269–283.
Bruno S, Cercignani M, Ron MA. White matter abnormalities in bipolar disorder: A voxel-based diffusion tensor imaging study. Bipolar Disord. 2008; 10: 460–468.
Buckner RL, Andrews-Hanna JR, Schacter DL. The brain's default network: Anatomy,function, and relevance to disease. Ann. N. Y. Acad. Sci. 2007; 1124: 1–42.
Buckner RL, Head D, Parker J, Fotenos AF, Marcus D, Morris JC, et al. A unified approach for morphometric and functional data analysis in young, old, and demented adults using automated atlas-based head size normalization: Reliability and validation against manual measurement of total intracranial volume. Neuroimage 2004; 23: 724–738.
Campanella S, Absil J, Carbia Sinde C, Schroder E, Peigneux P, Bourguignon M, et al. Neural correlates of correct and failed response inhibition in heavy versus light social drinkers: an fMRI study during a go/no-go task by healthy participants. Brain Imaging Behav. 2017; 11: 1796–1811.
Can A, Frost DO, Cachope R, Cheer JF, Gould TD. Chronic lithium treatment rectifies maladaptive dopamine release in the nucleus accumbens. J. Neurochem. 2016; 139: 576–585.
Carlesimo GA, Caltagirone C, Gainotti G. The Mental Deterioration Battery: normative data, diagnostic reliability and qualitative analyses of cognitive impairment. The Group for the Standardization of the Mental Deterioration Battery. Eur. Neurol. 1996; 36: 378–384.
Cassidy F, Ahearn EP, Carroll BJ. Substance abuse in bipolar disorder. Bipolar Disord. 2001; 3: 181–188.
Catani M, Dell'Acqua F, Thiebaut de Schotten M. A revised limbic system model for memory, emotion and behaviour. Neurosci. Biobehav. Rev. 2013; 37: 1724–1737.
Centorrino F, Fogarty K V., Sani G, Salvatore P, Cincotta SL, Hennen J, et al. Use of combinations of antipsychotics: McLean Hospital inpatients, 2002. Hum. Psychopharmacol. 2005; 20: 485–492.
Chan WY, Yang GL, Chia MY, Woon PS, Lee J, Keefe R, et al. Cortical and subcortical white matter abnormalities in adults with remitted first-episode mania revealed by Tract-Based Spatial Statistics. Bipolar Disord. 2010; 12: 383–389.
Chen HH, Nicoletti MA, Hatch JP, Sassi RB, Axelson D, Brambilla P, et al. Abnormal left superior temporal gyrus volumes in children and adolescents with bipolar disorder: A magnetic resonance imaging study. Neurosci. Lett. 2004; 363: 65–68.
Chepenik LG, Fredericks C, Papademetris X, Spencer L, Lacadie C, Wang F, et al. Effects of the brain-derived neurotrophic growth factor Val66Met variation on hippocampus morphology in bipolar disorder.

Neuropsychopharmacology 2009; 34: 944–951.
Chiapponi C, Piras F, Fagioli S, Girardi P, Caltagirone C, Spalletta G. Hippocampus age-related microstructural changes in schizophrenia: A case-control mean diffusivity study. Schizophr. Res. 2014; 157: 214–217.
Chiapponi C, De Rossi P, Piras F, Gili T, Spalletta G. Brain morphometry: Schizophrenia. In: Spalletta G, Piras F, Gili T, editor(s). Neuromethods. Springer; 2018. p. 323–338.
De Coene B, Hajnal J V, Gatehouse P, Longmore DB, White SJ, Oatridge A, et al. MR of the brain using fluid-attenuated inversion recovery (FLAIR) pulse sequences. AJNR. Am. J. Neuroradiol. 1992; 13: 1555–64.
Colla M, Schubert F, Bubner M, Heidenreich JO, Bajbouj M, Seifert F, et al. Glutamate as a spectroscopic marker of hippocampal structural plasticity is elevated in long-term euthymic bipolar patients on chronic lithium therapy and correlates inversely with diurnal cortisol. Mol. Psychiatry 2009; 14: 696–704.
Coque L, Mukherjee S, Cao JL, Spencer S, Marvin M, Falcon E, et al. Specific role of VTA dopamine neuronal firing rates and morphology in the reversal of anxiety-related, but not depression-related behavior in the clockδ19 mouse model of mania. Neuropsychopharmacology 2011; 36: 1478–1488.
Craddock N, Owen MJ. The beginning of the end for the Kraepelinian dichotomy. Br. J. Psychiatry 2005; 186: 364–366.
D'Esposito M, Aguirre GK, Zarahn E, Ballard D, Shin RK, Lease J. Functional MRI studies of spatial and nonspatial working memory. Cogn. Brain Res. 1998; 7: 1–13.
Davis KA, Kwon A, Cardenas VA, Deicken RF. Decreased cortical gray and cerebral white matter in male patients with familial bipolar I disorder. J. Affect. Disord. 2004; 82: 475–485.
Davis SW, Dennis NA, Buchler NG, White LE, Madden DJ, Cabeza R. Assessing the effects of age on long white matter tracts using diffusion tensor tractography. Neuroimage 2009; 46: 530–41.
De-Paula VJ, Gattaz WF, Forlenza O V. Long-term lithium treatment increases intracellular and extracellular brain-derived neurotrophic factor (BDNF) in cortical and hippocampal neurons at subtherapeutic concentrations. Bipolar Disord. 2016; 18: 692–695.
Deichmann R, Schwarzbauer C, Turner R. Optimisation of the 3D MDEFT sequence for anatomical brain imaging: Technical implications at 1.5 and 3 T. Neuroimage 2004; 21: 757–767.
Department of Health Statistics and Informatics. The Global Burden of Disease 2004 Update. 2008.
Devinsky O, Morrell MJ, Vogt BA, Dewinsky O, Morrell MJ, Vogt BA. Contributions of anterior cingulate cortex to behavior. Brain 1995; 118: 279–306.
Diedrichsen J, Balsters JH, Flavell J, Cussans E, Ramnani N. A probabilistic MR atlas of the human cerebellum. Neuroimage 2009; 46: 39–46.
Dixon JF, Hokin LE. Lithium acutely inhibits and chronically up-regulates and stabilizes glutamate uptake by presynaptic nerve endings in mouse cerebral cortex. Proc. Natl. Acad. Sci. 1998; 95: 8363–8368.

Doty TJ, Payne ME, Steffens DC, Beyer JL, Krishnan KRR, LaBar KS. Age-dependent reduction of amygdala volume in bipolar disorder. Psychiatry Res. - Neuroimaging 2008; 163: 84–94.
Dusi N, Delvecchio G, Rovera C, Altamura CA, Brambilla P. Voxel-Based Morphometry Imaging Studies in Major Depression. In: Spalletta G, Piras F, Gili T, editor(s). . Springer; 2018. p. 385–402.
Emsell L, Langan C, Van Hecke W, Barker GJ, Leemans A, Sunaert S, et al. White matter differences in euthymic bipolar I disorder: A combined magnetic resonance imaging and diffusion tensor imaging voxel-based study. Bipolar Disord. 2013; 15: 365–376.
Erdfelder E, Faul F, Buchner A, Lang AA-G, Franz Faul Edgar Erdfelder and Albert-georg Lang and Axel Buchner. Statistical power analyses using G*Power 3.1: test for correlation and regression analyses. Behav. Res. Methods 2009; 41: 1149–1160.
van Erp TGM, Thompson PM, Kieseppä T, Bearden CE, Marino AC, Hoftman GD, et al. Hippocampal morphology in lithium and non-lithium-treated bipolar I disorder patients, non-bipolar co-twins, and control twins. Hum. Brain Mapp. 2012; 33: 501–510.
Etain B, Henry C, Bellivier F, Mathieu F, Leboyer M. Beyond genetics: Childhood affective trauma in bipolar disorder. Bipolar Disord. 2008; 10: 867–876.
Fatemi SH, Folsom TD. The neurodevelopmental hypothesis of Schizophrenia, revisited. Schizophr. Bull. 2009; 35: 528–548.
First M, Gibbon M, Spitzer R. Structured Clinical Interview for DSM-IV Axis II Personality Disorders (SCID-II). Am. Psychiatr. Press. Inc. 1997
First MB et, Spitzer RL, Gibbon M, Williams JBW. Structured Clinical Interview for DSM-IV-TR Axis I Disorders, Research Version, Non-patient Edition. 2002.
First MB, Gibbon M, Spitzer RL, Williams JB, Benjamin L. Structured Clinical Interview for DSM-IV Axis II Personality Disorders, (SCID-II). Washington DC: American Psychiatric Press, Inc.; 1997.
First MB, Spitzer RL, Gibbon M, Williams JBW. Structured Clinical Interview for DSM-IV-TR Axis I Disorders, Patient Edition (SCID-I/P, 11/2002 revision). 2002.
Fischl B, Salat DH, Busa E, Albert M, Dieterich M, Haselgrove C, et al. Whole brain segmentation: Automated labeling of neuroanatomical structures in the human brain. Neuron 2002; 33: 341–355.
Fischl B, Salat DH, Van Der Kouwe AJW, Makris N, Ségonne F, Quinn BT, et al. Sequence-independent segmentation of magnetic resonance images. In: NeuroImage. 2004.
Floresco SB. The Nucleus Accumbens: An Interface Between Cognition, Emotion, and Action. Annu. Rev. Psychol. 2015; 66: 25–52.
Foland-Ross LC, Brooks JO, Mintz J, Bartzokis G, Townsend J, Thompson PM, et al. Mood-state effects on amygdala volume in bipolar disorder. J. Affect. Disord. 2012; 139: 298–301.
Foland-Ross LC, Thompson PM, Sugar CA, Madsen SK, Shen JK, Penfold C, et al. Investigation of cortical thickness abnormalities in lithium-free adults

with bipolar I disorder using cortical pattern matching. Am. J. Psychiatry 2011; 168: 530–539.
Foland LC, Altshuler LL, Sugar CA, Lee AD, Leow AD, Townsend J, et al. Increased volume of the amygdala and hippocampus in bipolar patients treated with lithium. Neuroreport 2008; 19: 221–224.
Folstein MF, Folstein SE, McHugh PR. 'Mini-mental state'. J. Psychiatr. Res. 1975a; 12: 189–198.
Folstein MF, Folstein SE, McHugh PR. 'Mini-mental state'. J. Psychiatr. Res. 1975b; 12: 189–198.
Frey BN, Zunta-Soares GB, Caetano SC, Nicoletti MA, Hatch JP, Brambilla P, et al. Illness duration and total brain gray matter in bipolar disorder: Evidence for neurodegeneration? Eur. Neuropsychopharmacol. 2008; 18: 717–722.
Fukuoka H, Hirai T, Okuda T, Shigematsu Y, Sasao A, Kimura E, et al. Comparison of the added value of contrast-enhanced 3D fluid-attenuated inversion recovery and magnetization-prepared rapid acquisition of gradient echo sequences in relation to conventional postcontrast T1-weighted images for the evaluation of leptomening. Am. J. Neuroradiol. 2010; 31: 868–873.
Fusar-Poli P, Allen P, McGuire P. Egas Moniz (1875-1955), the father of psychosurgery. Br. J. Psychiatry 2008; 193: 50.
Ganzetti M, Wenderoth N, Mantini D. Mapping pathological changes in brain structure by combining T1- and T2-weighted MR imaging data. Neuroradiology 2015; 57: 917–28.
Gardner HH, Kleinman NL, Brook RA, Rajagopalan K, Brizee TJ, Smeeding JE. The economic impact of bipolar disorder in an employed population from an employer perspective. J. Clin. Psychiatry 2006; 67: 1209–1218.
Geddes JR, Burgess S, Hawton K, Jamison K, Goodwin GM. Long-term lithium therapy for bipolar disorder: systematic review and meta-analysis of randomized controlled trials. [Internet]. Am. J. Psychiatry 2004; 161: 217–22.Available from: http://www.ncbi.nlm.nih.gov/pubmed/14754766
Germaná C, Kempton MJ, Sarnicola A, Christodoulou T, Haldane M, Hadjulis M, et al. The effects of lithium and anticonvulsants on brain structure in bipolar disorder. Acta Psychiatr. Scand. 2010; 122: 481–487.
Geva T. Magnetic resonance imaging: historical perspective. J. Cardiovasc. Magn. Reson. 2006; 8: 573–580.
Giakoumatos CI, Nanda P, Mathew IT, Tandon N, Shah J, Bishop JR, et al. Effects of lithium on cortical thickness and hippocampal subfield volumes in psychotic bipolar disorder [Internet]. J. Psychiatr. Res. 2015; 61: 180–187.[cited 2018 Oct 10] Available from: https://www.sciencedirect.com/science/article/pii/S0022395614003495
Giedd JN, Blumenthal J, Jeffries NO, Castellanos FX, Liu H, Zijdenbos A, et al. Brain development during childhood and adolescence: a longitudinal MRI study. Nat. Neurosci. 1999; 2: 861–863.
Gigante AD, Young LT, Yatham LN, Andreazza AC, Nery FG, Grinberg LT, et al. Morphometric post-mortem studies in bipolar disorder: Possible association with oxidative stress and apoptosis. Int. J. Neuropsychopharmacol. 2011; 14: 1075–1089.
Goodwin F, Jamison KR. Manic-Depressive Illness: Bipolar Disorders and

Recurrent Depression. 2012.
Graham J, Salimi-Khorshidi G, Hagan C, Walsh N, Goodyer I, Lennox B, et al. Meta-analytic evidence for neuroimaging models of depression: State or trait? J. Affect. Disord. 2013; 151: 423–431.
Gray JD, Mcewen BS. Lithium's role in neural plasticity and its implications for mood disorders. Acta Psychiatr. Scand. 2013; 128: 347–361.
Greimel E, Nehrkorn B, Schulte-Rüther M, Fink GR, Nickl-Jockschat T, Herpertz-Dahlmann B, et al. Changes in grey matter development in autism spectrum disorder. Brain Struct. Funct. 2013; 218: 929–942.
Groenewegen HJ, Wright CI, Beijer AVJ. Chapter 29 The nucleus accumbens: gateway for limbic structures to reach the motor system? In: Progress in Brain Research. 1996. p. 485–511.
Gulseren S, Gurcan M, Gulseren L, Gelal F, Erol A. T2 hyperintensities in bipolar patients and their healthy siblings. Arch. Med. Res. 2006; 37: 79–85.
Hafeman DM, Chang KD, Garrett AS, Sanders EM, Phillips ML. Effects of medication on neuroimaging findings in bipolar disorder: An updated review. Bipolar Disord. 2012; 14: 375–410.
Hagan CC, Graham JME, Tait R, Widmer B, Van Nieuwenhuizen AO, Ooi C, et al. Adolescents with current major depressive disorder show dissimilar patterns of age-related differences in ACC and thalamus. NeuroImage Clin. 2015; 7: 391–399.
Hajek T, Cullis J, Novak T, Kopecek M, Höschl C, Blagdon R, et al. Hippocampal volumes in bipolar disorders: Opposing effects of illness burden and lithium treatment. Bipolar Disord. 2012; 14: 261–270.
Hajek T, Kopecek M, Höschl C, Alda M. Smaller hippocampal volumes in patients with bipolar disorder are masked by exposure to lithium: A meta-analysis. J. Psychiatry Neurosci. 2012; 37: 333–343.
Hallahan B, Newell J, Soares JC, Brambilla P, Strakowski SM, Fleck DE, et al. Structural magnetic resonance imaging in bipolar disorder: An international collaborative mega-analysis of individual adult patient data. Biol. Psychiatry 2011; 69: 326–335.
Haller S, Xekardaki A, Delaloye C, Canuto A, Lövblad KO, Gold G, et al. Combined analysis of grey matter voxel-based morphometry and white matter tract-based spatial statistics in late-life bipolar disorder. J. Psychiatry Neurosci. 2011; 36: 391–401.
Hamilton M. A rating scale for depression. J. Neurol. Neurosurg. Psychiatry 1960; 23: 56–62.
Hartberg CB, Jørgensen KN, Haukvik UK, Westlye LT, Melle I, Andreassen OA, et al. Lithium treatment and hippocampal subfields and amygdala volumes in bipolar disorder. Bipolar Disord. 2015; 17: 496–506.
Hercher C, Turecki G, Mechawar N. Through the looking glass: Examining neuroanatomical evidence for cellular alterations in major depression. J. Psychiatr. Res. 2009; 43: 947–961.
Herrero MT, Barcia C, Navarro JM. Functional anatomy of thalamus and basal ganglia. Child's Nerv. Syst. 2002; 18: 386–404.
Hibar DP, Westlye LT, van Erp TGM, Rasmussen J, Leonardo CD, Faskowitz J, et al. Subcortical volumetric abnormalities in bipolar disorder. Mol.

Psychiatry 2016: 1–7.
Higashitani Y, Kudo Y, Ogura A, Kato H. Acute effects of lithium on synaptic transmission in rat hippocampus studied in vitro. Biol. Psychiatry 1990; 27: 174–182.
Hirschfeld RMA, Lewis L, Vornik LA. Perceptions and impact of bipolar disorder: How far have we really come? Results of the National Depressive and Manic-Depressive Association 2000 Survey of individuals with bipolar disorder. J. Clin. Psychiatry 2003; 64: 161–174.
Hoppenbrouwers SS, Schutter DJLG, Fitzgerald PB, Chen R, Daskalakis ZJ. The role of the cerebellum in the pathophysiology and treatment of neuropsychiatric disorders: a review. Brain Res Rev 2008; 59: 185–200.
Hwang J, In KL, Dager SR, Friedman SD, Jung SO, Jun YL, et al. Basal ganglia shape alterations in bipolar disorder. Am. J. Psychiatry 2006; 163: 276–285.
Ikegaya Y, Saito H, Abe K. High-frequency stimulation of the basolateral amygdala facilitates the induction of long-term potentiation in the dentate gyrus in vivo. Neurosci. Res. 1995; 22: 203–207.
Iorio M, Spalletta G, Chiapponi C, Luccichenti G, Cacciari C, Orfei MD, et al. White matter hyperintensities segmentation: A new semi-automated method. Front. Aging Neurosci. 2013; 5
Janiri D, Ambrosi E, Danese E, Panaccione I, Simonetti A, Sani G. Bipolar Disorders. In: Spalletta G, Piras F, Gili T, editor(s). . Springer; 2018. p. 339–383.
Janiri D, Sani G, Danese E, Simonetti A, Ambrosi E, Angeletti G, et al. Childhood traumatic experiences of patients with bipolar disorder type i and type II. J. Affect. Disord. 2015; 175: 92–97.
Janiri D, Sani G, Rossi P De, Piras F, Iorio M, Banaj N, et al. Amygdala and hippocampus volumes are differently affected by childhood trauma in patients with bipolar disorders and healthy controls. Bipolar Disord. 2017; 19: 353–362.
Job DE, Whalley HC, McConnell S, Glabus M, Johnstone EC, Lawrie SM. Voxel-based morphometry of grey matter densities in subjects at high risk of schizophrenia. Schizophr.Res. 2003; 64: 1–13.
Johansen-Berg H, Johansen-Berg H, Behrens TEJ, Behrens TEJ, Robson MD, Robson MD, et al. Changes in connectivity profiles define functionally distinct regions in human medial frontal cortex. Proc. Natl. Acad. Sci. U. S. A. 2004; 101: 13335–40.
Johnson SA, Wang JF, Sun X, McEwen BS, Chattarji S, Young LT. Lithium treatment prevents stress-induced dendritic remodeling in the rodent amygdala. Neuroscience 2009; 163: 34–39.
Johnstone E, Frith CD, Crow TJ, Husband J, Kreel L. Cerebral Ventricular Size and Cognitive Impairment in Chronic Schizophrenia. Lancet 1976; 308: 924–926.
Jones DK, Leemans A. Diffusion Tensor Imaging. Methods Mol. Biol. 2011; 711: 127–144.
Jovicich J, Czanner S, Han X, Salat D, van der Kouwe A, Quinn B, et al. MRI-derived measurements of human subcortical, ventricular and intracranial brain volumes: Reliability effects of scan sessions, acquisition sequences,

data analyses, scanner upgrade, scanner vendors and field strengths. Neuroimage 2009; 46: 177–192.
Kafantaris V, Kingsley P, Ardekani B, Saito E, Lencz T, Lim K, et al. Lower orbital frontal white matter integrity in adolescents with bipolar I disorder. J. Am. Acad. Child Adolesc. Psychiatry 2009; 48: 79–86.
Kalmar JH, Wang F, Spencer L, Edmiston E, Lacadie CM, Martin A, et al. Preliminary evidence for progressive prefrontal abnormalities in adolescents and young adults with bipolar disorder. J. Int. Neuropsychol. Soc. 2009; 15: 476–481.
Kaur S, Sassi RB, Axelson D, Nicoletti M, Brambilla P, Monkul ES, et al. Cingulate cortex anatomical abnormalities in children and adolescents with bipolar disorder. Am. J. Psychiatry 2005; 162: 1637–43.
Kempton MJ, Geddes JR, Ettinger U, Williams SCR, Grasby PM. Meta-analysis, database, and meta-regression of 98 structural imaging studies in bipolar disorder. Arch. Gen. Psychiatry 2008; 65: 1017–1032.
Kempton MJ, Haldane M, Jogia J, Grasby PM, Collier D, Frangou S. Dissociable Brain Structural Changes Associated with Predisposition, Resilience, and Disease Expression in Bipolar Disorder [Internet]. J. Neurosci. 2009; 29: 10863–10868.Available from: http://www.jneurosci.org/cgi/doi/10.1523/JNEUROSCI.2204-09.2009
Kempton MJ, Salvado Z, Munafò MR, Geddes JR, Simmons A, Frangou S, et al. Structural neuroimaging studies in major depressive disorder. Meta-analysis and comparison with bipolar disorder. Arch. Gen. Psychiatry 2011; 68: 675–690.
Kikinis R, Pieper SD, Vosburgh KG. 3D Slicer: A Platform for Subject- Specific Image Analysis, Visualization, and Clinical Support. Intraoperative Imaging Image-Guided Ther. 2014: 277–289.
Kilgore EJ, Elster AD. Walter Dandy and the history of ventriculography. Radiology 1995; 194: 657–60.
Kim D, Cho HB, Dager SR, Yurgelun-Todd DA, Yoon S, Lee JH, et al. Posterior cerebellar vermal deficits in bipolar disorder. J. Affect. Disord. 2013; 150: 499–506.
Kraepelin E. Manic-Depressive Insanity and Paranoia. Igarss 2014 2014: 1–5.
Kropf D, Muller-Oerlinghausen B. Changes in learning, memory, and mood during lithium treatment. Approach to a research strategy. Acta Psychiatr Scand 1979; 59: 97–124.
Laidi C, d'Albis MA, Wessa M, Linke J, Phillips ML, Delavest M, et al. Cerebellar volume in schizophrenia and bipolar I disorder with and without psychotic features. Acta Psychiatr. Scand. 2015; 131: 223–233.
Lazar M, Weinstein DM, Tsuruda JS, Hasan KM, Arfanakis K, Meyerand ME, et al. White matter tractography using diffusion tensor deflection. Hum. Brain Mapp. 2003; 18: 306–321.
Leech R, Sharp DJ. The role of the posterior cingulate cortex in cognition and disease. Brain 2014; 137: 12–32.
Lewis SW, Murray RM. Obstetric complications, neurodevelopmental deviance, and risk of schizophrenia. J. Psychiatr. Res. 1987; 21: 413–421.
Liberg B, Ekman CJ, Sellgren C, Johansson A, Landén M. Vertex-based

morphometry in euthymic bipolar disorder implicates striatal regions involved in psychomotor function. Psychiatry Res. - Neuroimaging 2014; 221: 173–178.
Ligon BL. Biography: history of developments in imaging techniques: Egas Moniz and angiography. Semin. Pediatr. Infect. Dis. 2003; 14: 173–181.
Lim CS, Baldessarini RJ, Vieta E, Yucel M, Bora E, Sim K. Longitudinal neuroimaging and neuropsychological changes in bipolar disorder patients: Review of the evidence. Neurosci. Biobehav. Rev. 2013; 37: 418–435.
Lipp I, Muhlert N, Tomassini V. Brain Morphometry in Multiple Sclerosis. In: Spalletta G, Piras F, Gili T, editor(s). . Springer; 2018. p. 279–300.
Liu JX, Chen YS, Hsieh JC, Su TP, Yeh TC, Chen LF. Differences in white matter abnormalities between bipolar I and II disorders. J Affect Disord 2010; 127: 309–315.
López-Jaramillo C, Vargas C, Díaz-Zuluaga AM, Palacio JD, Castrillón G, Bearden C, et al. Increased hippocampal, thalamus and amygdala volume in long-term lithium-treated bipolar I disorder patients compared with unmedicated patients and healthy subjects. Bipolar Disord. 2017; 19: 41–49.
Lopez-Larson M, Breeze JL, Kennedy DN, Hodge SM, Tang L, Moore C, et al. Age-related changes in the corpus callosum in early-onset bipolar disorder assessed using volumetric and cross-sectional measurements. Brain Imaging Behav. 2010; 4: 220–231.
López-Larson MP, DelBello MP, Zimmerman ME, Schwiers ML, Strakowski SM. Regional prefrontal gray and white matter abnormalities in bipolar disorder. Biol. Psychiatry 2002; 52: 93–100.
Lu LH, Zhou XJ, Keedy SK, Reilly JL, Sweeney JA. White matter microstructure in untreated first episode bipolar disorder with psychosis: Comparison with schizophrenia. Bipolar Disord. 2011; 13: 604–613.
Lyoo IK, Kim MJ, Stoll AL, Demopulos CM, Parow AM, Dager SR, et al. Frontal lobe gray matter density decreases in bipolar I disorder. Biol. Psychiatry 2004; 55: 648–651.
Lyoo IK, Lee HK, Jung JH, Noam GG, Renshaw PF. White matter hyperintensities on magnetic resonance imaging of the brain in children with psychiatric disorders. Compr. Psychiatry 2002; 43: 361–368.
Mahon K, Burdick KE, Szeszko PR. A role for white matter abnormalities in the pathophysiology of bipolar disorder. Neurosci. Biobehav. Rev. 2010; 34: 533–554.
Mahon K, Wu J, Malhotra AK, Burdick KE, DeRosse P, Ardekani BA, et al. A voxel-based diffusion tensor imaging study of white matter in bipolar disorder. Neuropsychopharmacology 2009; 34: 1590–1600.
Malhi GS, Tanious M, Das P, Coulston CM, Berk M. Potential mechanisms of action of lithium in bipolar disorder: Current understanding. CNS Drugs 2013; 27: 135–153.
Mamah D, Alpert KI, Barch DM, Csernansky JG, Wang L. Subcortical neuromorphometry in schizophrenia spectrum and bipolar disorders. NeuroImage. Clin. 2016; 11: 276–86.
Mamah D, Barch DM, Csernansky JG. Neuromorphometric Measures as Endophenotypes of Schizophrenia Spectrum Disorders. Handb.

Neuropsychiatr. Biomarkers, Endophenotypes Genes, 2009: 87–122.
Manji HK, Moore GJ, Chen G. Clinical and preclinical evidence for the neurotrophic effects of mood stabilizers: Implications for the pathophysiology and treatment of manic-depressive illness. Biol. Psychiatry 2000; 48: 740–754.
De Marco M, Venneri A. Brain Morphometry: Alzheimer's Disease. In: Spalletta G, Piras F, Gili T, editor(s). . Springer; 2018. p. 217–240.
Maruta S, Suzuki E, Yokoyama M, Sato T, Inada K, Watanabe S, et al. Effects of intraperitoneally injected lithium, imipramine and diazepam on nitrate levels in rat amygdala. Psychiatry Clin. Neurosci. 2005; 59: 358–361.
Matsuda H. Morphometry in Normal Aging. In: Spalletta G, Piras F, Gili T, editor(s). . Springer; 2018. p. 165–181.
Matsusue E, Sugihara S, Fujii S, Ohama E, Kinoshita T, Ogawa T. White matter changes in elderly people: MR-pathologic correlations. Magn. Reson. Med. Sci. 2006; 5: 99–104.
Mavridis I, Boviatsis E, Anagnostopoulou S. The human nucleus accumbens suffers parkinsonism-related shrinkage: A novel finding. Surg. Radiol. Anat. 2011; 33: 595–599.
Mayberg HS. Neuroimaging and Psychiatry: The Long Road from Bench to Bedside. Hastings Cent. Rep. 2014; 44
McDonald C, Author A, National University of I, Galway GI, Correspondence A, C. McDonald NU of IGGI. Brain structural effects of psychopharmacological treatment in bipolar disorder. Curr Neuropharmacol 2015; 13: 445–457.
McDonald C, Bullmore E, Sham P, Chitnis X, Suckling J, MacCabe J, et al. Regional volume deviations of brain structure in schizophrenia and psychotic bipolar disorder: Computational morphometry study. Br. J. Psychiatry 2005; 186: 369–377.
McDonald C, Zanelli J, Rabe-Hesketh S, Ellison-Wright I, Sham P, Kalidindi S, et al. Meta-analysis of magnetic resonance imaging brain morphometry studies in bipolar disorder. Biol. Psychiatry 2004; 56: 411–417.
Measso, G., Cavarzeran, F., Zappalà, G., Lebowitz, B. D., Crook, T. H., Pirozzolo, F. J., ... & Grigoletto F. The mini-mental state examination: Normative study of an Italian random sample. Dev. Neuropsychol. 1993; 9: 77–85.
Mechelli A, Price CJ, Friston KJ, Ashburner J. Voxel-based morphometry of the human brain: methods and applications. Curr. Med. … 2005; 1: 105–113.
Mega MS, Cummings JL, Salloway S, Malloy P. The limbic system: an anatomic, phylogenetic, and clinical perspective. J. Neuropsychiatry Clin. Neurosci. 1997; 9: 315–330.
Melhem ER, Mori S, Mukundan G, Kraut MA, Pomper MG, van Zijl PCM. Diffusion Tensor MR Imaging of the Brain and White Matter Tractography. Am. J. Roentgenol. 2002; 178: 3–16.
Michèle W, Josselin H, Marion L, Sandra C, Cyril P, Jean-Luc M, et al. Microstructural white matter changes in euthymic bipolar patients: a whole-brain diffusion tensor imaging study. Bipolar Disord. 2009; 11: 504–514.
Mills NP, DelBello MP, Adler CM, Strakowski SM. MRI analysis of cerebellar

vermal abnormalities in bipolar disorder. Am. J. Psychiatry 2005; 162: 1530–1532.
Monkul ES, Matsuo K, Nicoletti MA, Dierschke N, Hatch JP, Dalwani M, et al. Prefrontal gray matter increases in healthy individuals after lithium treatment: A voxel-based morphometry study. Neurosci. Lett. 2007; 429: 7–11.
Montgomery BJ. CT scanning recognized with Nobel Prize. J. Am. Med. Assoc. 1979; 242: 2380.
Moore GJ, Bebchuk JM, Wilds IB, Chen G, Menji HK. Lithium-induced increase in human brain grey matter. Lancet 2000; 356: 1241–1242.
Moore GJ, Cortese BM, Glitz DA, Zajac-Benitez C, Quiroz JA, Uhde TW, et al. A longitudinal study of the effects of lithium treatment on prefrontal and subgenual prefrontal gray matter volume in treatment-responsive bipolar disorder patients. J. Clin. Psychiatry 2009; 70: 699–705.
Morey RA, Petty CM, Xu Y, Pannu Hayes J, Wagner HR, Lewis D V., et al. A comparison of automated segmentation and manual tracing for quantifying hippocampal and amygdala volumes. Neuroimage 2009; 45: 855–866.
Mori S, Zhang J. Principles of Diffusion Tensor Imaging and Its Applications to Basic Neuroscience Research. Neuron 2006; 51: 527–539.
Mori S, van Zijl PCM. Fiber tracking: principles and strategies - a technical review. NMR Biomed. 2002; 15: 468–480.
Morita T, Asada M, Naito E. Contribution of Neuroimaging Studies to Understanding Development of Human Cognitive Brain Functions. Front. Hum. Neurosci. 2016; 10: 1–14.
Naranjo CA, Tremblay LK, Busto UE. The role of the brain reward system in depression. Prog. Neuro-Psychopharmacology Biol. Psychiatry 2001; 25: 781–823.
Nestler EJ, Carlezon WA. The Mesolimbic Dopamine Reward Circuit in Depression. Biol. Psychiatry 2006; 59: 1151–1159.
Ng WXD, Lau IY, Graham S, Sim K. Neurobiological evidence for thalamic, hippocampal and related glutamatergic abnormalities in bipolar disorder: A review and synthesis. Neurosci. Biobehav. Rev. 2009; 33: 336–354.
Nichols TE, Holmes AP. Nonparametric permutation tests for functional neuroimaging: A primer with examples. Hum. Brain Mapp. 2002; 15: 1–25.
Nugent AC, Milham MP, Bain EE, Mah L, Cannon DM, Marrett S, et al. Cortical abnormalities in bipolar disorder investigated with MRI and voxel-based morphometry. Neuroimage 2006; 30: 485–497.
Ogawa S, Lee TM, Kay AR, Tank DW. Brain magnetic resonance imaging with contrast dependent on blood oxygenation. Proc. Natl. Acad. Sci. U. S. A. 1990; 87: 9868–72.
Ong D, Walterfang M, Malhi GS, Styner M, Velakoulis D, Pantelis C. Size and shape of the caudate nucleus in individuals with bipolar affective disorder. Aust. N. Z. J. Psychiatry 2012; 46: 340–51.
Oostervink F, Nolen WA, Kok RM. Two years' outcome of acute mania in bipolar disorder: Different effects of age and age of onset. Int. J. Geriatr. Psychiatry 2015; 30: 201–209.
Paillère Martinot ML, Lemaitre H, Artiges E, Miranda R, Goodman R, Penttilä J,

et al. White-matter microstructure and gray-matter volumes in adolescents with subthreshold bipolar symptoms. Mol. Psychiatry 2014; 19: 462–470.
Di Paola M, Bourisly AK. Structural MRI in Neurodegenerative Non-Alzheimer's Dementia. In: Spalletta G, Piras F, Gili T, editor(s). . Springer; 2018. p. 241–265.
Parker G, Hadzi-Pavlovic D, Wilhelm K, Hickie I, Brodaty H, Boyce P, et al. Defining melancholia: Properties of a refined sign-based measure. Br. J. Psychiatry 1994; 164: 316–326.
Patenaude B, Smith SM, Kennedy DN, Jenkinson M. A Bayesian model of shape and appearance for subcortical brain segmentation. Neuroimage 2011; 56: 907–922.
Péran P, Nemmi F, Barbagallo G. Brain Morphometry: Parkinson's Disease. In: Spalletta G, Piras F, Gili T, editor(s). . Springer; 2018. p. 267–277.
Phan KL, Wager T, Taylor SF, Liberzon I. Functional neuroanatomy of emotion: A meta-analysis of emotion activation studies in PET and fMRI. Neuroimage 2002; 16: 331–348.
Phillips ML, Drevets WC, Rauch SL, Lane R. Neurobiology of emotion perception II: Implications for major psychiatric disorders. Biol. Psychiatry 2003; 54: 515–528.
Phillips ML, Swartz HA. A critical appraisal of neuroimaging studies of bipolar disorder: toward a new conceptualization of underlying neural circuitry and a road map for future research of neuroimaging studies of bipolar disorder: toward a new conceptualization of underlying ne. Am. J. Psychiatry 2014: 829–843.
Pincock S. US and UK researchers share Nobel prize. Paul C Lauterbur and Peter Mansfield share award for seminal work on MRI. Lancet (London, England) 2003; 362: 1203.
Pizzagalli DA, Sherwood RJ, Henriques JB, Davidson RJ. Frontal brain asymmetry and reward responsiveness: A source-localization study. Psychol. Sci. 2005; 16: 805–813.
Pompili M, Ehrlich S, De Pisa E, Mann JJ, Innamorati M, Cittadini A, et al. White matter hyperintensities and their associations with suicidality in patients with major affective disorders. Eur. Arch. Psychiatry Clin. Neurosci. 2007; 257: 494–499.
Quigley SJ, Scanlon C, Kilmartin L, Emsell L, Langan C, Hallahan B, et al. Volume and shape analysis of subcortical brain structures and ventricles in euthymic bipolar I disorder. Psychiatry Res. - Neuroimaging 2015; 233: 324–330.
Quiroz JA, MacHado-Vieira R, Zarate CA, Manji HK. Novel insights into lithium's mechanism of action: Neurotrophic and neuroprotective effects. Neuropsychobiology 2010; 62: 50–60.
Radenbach K, Flaig V, Schneider-Axmann T, Usher J, Reith W, Falkai P, et al. Thalamic volumes in patients with bipolar disorder. Eur. Arch. Psychiatry Clin. Neurosci. 2010; 260: 601–607.
Raichle ME. A brief history of human brain mapping. Trends Neurosci. 2009; 32: 118–126.
Raju TN. The Nobel chronicles. 1976: Baruch S Blumberg (b 1925); Daniel

Carleton Gajdusek (1923). Lancet (London, England) 1999; 354: 1394.
Rimol LM, Hartberg CB, Nesvåg R, Fennema-Notestine C, Hagler DJ, Pung CJ, et al. Cortical Thickness and Subcortical Volumes in Schizophrenia and Bipolar Disorder. Biol. Psychiatry 2010; 68: 41–50.
Rodriguez AO. Principles of magnetic resonance imaging. Rev. Mex. Fis. 2004; 50: 272–286.
Roozendaal B, Phillips RG, Power AE, Brooke SM, Sapolsky RM, McGaugh JL. Memory retrieval impairment induced by hippocampal CA3 lesions is blocked by adrenocortical suppression. Nat. Neurosci. 2001; 4: 1169–1171.
Rosen C, Marvin R, Reilly JL, DeLeon O, Harris MSH, Keedy SK, et al. Phenomenology of first-episode psychosis in schizophrenia, bipolardisorder, and unipolar depression: A comparative analysis. Clin. Schizophr. Relat. Psychoses 2012; 6
Rubinov M, Sporns O. Complex network measures of brain connectivity: Uses and interpretations. Neuroimage 2010; 52: 1059–1069.
Sampath P, Long DM, Brem H, Yasui T. The Hunterian Neurosurgical Laboratory: The first 100 years of neurosurgical research. Neurosurgery 2000; 46: 184–195.
Sanfilipo MP, Benedict RHB, Zivadinov R, Bakshi R. Correction for intracranial volume in analysis of whole brain atrophy in multiple sclerosis: The proportion vs. residual method. Neuroimage 2004; 22: 1732–1743.
Sani G, Napoletano F, Vöhringer PA, Sullivan M, Simonetti A, Koukopoulos A, et al. Mixed depression: Clinical features and predictors of its onset associated with antidepressant use. Psychother. Psychosom. 2014; 83: 213–221.
Sassi RB, Brambilla P, Hatch JP, Nicoletti MA, Mallinger AG, Frank E, et al. Reduced left anterior cingulate volumes in untreated bipolar patients. Biol. Psychiatry 2004; 56: 467–475.
Sati P, George IC, Shea CD, Gaitán MI, Reich DS. FLAIR*: A Combined MR Contrast Technique for Visualizing White Matter Lesions and Parenchymal Veins. Radiology 2012; 265: 926–932.
Satterthwaite TD, Kable JW, Vandekar L, Katchmar N, Bassett DS, Baldassano CF, et al. Common and Dissociable Dysfunction of the Reward System in Bipolar and Unipolar Depression. Neuropsychopharmacology 2015; 40: 2258–2268.
Savitz J, Nugent AC, Bogers W, Liu A, Sills R, Luckenbaugh DA, et al. Amygdala volume in depressed patients with bipolar disorder assessed using high resolution 3T MRI: The impact of medication. Neuroimage 2010; 49: 2966–2976.
Scherk H, Kemmer C, Usher J, Reith W, Falkai P, Gruber O. No change to grey and white matter volumes in bipolar I disorder patients. Eur. Arch. Psychiatry Clin. Neurosci. 2008; 258: 345–349.
Schilling KG, Nath V, Blaber J, Harrigan RL, Ding Z, Anderson AW, et al. Effects of b-Value and Number of Gradient Directions on Diffusion MRI Measures Obtained with Q-ball Imaging. Proc. SPIE--the Int. Soc. Opt. Eng. 2017; 10133
Schrader DS, Bernasconi N, Bernasconi A. Brain Morphometry: Epilepsy. In:

Spalletta G, Piras F, Gili T, editor(s). . Springer; 2018. p. 301–321.
Selek S, Nicoletti M, Zunta-Soares GB, Hatch JP, Nery FG, Matsuo K, et al. A longitudinal study of fronto-limbic brain structures in patients with bipolar i disorder during lithium treatment. J. Affect. Disord. 2013; 150: 629–633.
Selvaraj S, Arnone D, Job D, Stanfield A, Farrow TFD, Nugent AC, et al. Grey matter differences in bipolar disorder: A meta-analysis of voxel-based morphometry studies. Bipolar Disord. 2012; 14: 135–145.
Shaltiel G, Chen G, Manji HK. Neurotrophic signaling cascades in the pathophysiology and treatment of bipolar disorder. Curr. Opin. Pharmacol. 2007; 7: 22–26.
Silverstone T, McPherson H, Li Q, Doyle T. Deep white matter hyperintensities in patients with bipolar depression, unipolar depression and age-matched control subjects. Bipolar Disord. 2003; 5: 53–57.
Simon NM, Otto MW, Wisniewski SR, Fossey M, Sagduyu K, Frank E, et al. Anxiety disorder comorbidity in bipolar disorder patients: Data from the first 500 participants in the Systematic Treatment Enhancement Program for Bipolar Disorder (STEP-BD). Am. J. Psychiatry 2004; 161: 2222–2229.
Simonetti A, Sani G, Dacquino C, Piras F, De Rossi P, Caltagirone C, et al. Hippocampal subfield volumes in short- and long-term lithium-treated patients with bipolar I disorder. Bipolar Disord. 2016; 18
Simonetti A, Sani G, Dacquino C, Piras F, De Rossi P, Caltagirone C, et al. Hippocampal subfield volumes in short- and long-term lithium-treated patients with bipolar I disorder. Bipolar Disord. 2016; 18: 352–362.
Smith SM, Nichols TE. Threshold-free cluster enhancement: Addressing problems of smoothing, threshold dependence and localisation in cluster inference. Neuroimage 2009; 44: 83–98.
Soares JC, Mann JJ. The functional neuroanatomy of mood disorders. J. Psychiatr. Res. 1997; 31: 393–432.
Spalletta G, Piras F, Gili T. Brain morphometry. Springer; 2018.
Spencer MD, Moorhead TWJ, McIntosh AM, Stanfield AC, Muir WJ, Hoare P, et al. Grey matter correlates of early psychotic symptoms in adolescents at enhanced risk of psychosis: A voxel-based study. Neuroimage 2007; 35: 1181–1191.
Sprooten E, Sussmann JE, Clugston A, Peel A, McKirdy J, Moorhead TWJ, et al. White matter integrity in individuals at high genetic risk of bipolar disorder. Biol. Psychiatry 2011; 70: 350–356.
Strakowski SM, Delbello MP, Adler CM. The functional neuroanatomy of bipolar disorder: a review of neuroimaging findings. Mol. Psychiatry 2005; 10: 105–16.
Strakowski SM, Fleck DE, Welge J, Eliassen JC, Norris M, Durling M, et al. fMRI brain activation changes following treatment of a first bipolar manic episode. Bipolar Disord. 2016; 18: 490–501.
Sussmann JE, Lymer GK, McKirdy J, Moorhead TW, Munoz Maniega S, Job D, et al. White matter abnormalities in bipolar disorder and schizophrenia detected using diffusion tensor magnetic resonance imaging. Bipolar Disord. 2009; 11: 11–18.
Symms M, Jäger HR, Schmierer K, Yousry TA. A review of structural magnetic

resonance neuroimaging. J. Neurol. Neurosurg. Psychiatry 2004; 75: 1235–1244.
Tamnes CK, Østby Y. Morphometry and Development: Changes in Brain Structure from Birth to Adult Age. In: Spalletta G, Piras F, Gili T, editor(s). . Springer; 2018. p. 143–164.
Usher J, Menzel P, Schneider-Axmann T, Kemmer C, Reith W, Falkai P, et al. Increased right amygdala volume in lithium-treated patients with bipolar i disorder. Acta Psychiatr. Scand. 2010; 121: 119–124.
Vederine FE, Wessa M, Leboyer M, Houenou J. A meta-analysis of whole-brain diffusion tensor imaging studies in bipolar disorder. Prog. Neuro-Psychopharmacology Biol. Psychiatry 2011; 35: 1820–1826.
Vieta E, Suppes T. Bipolar II disorder: Arguments for and against a distinct diagnostic entity. Bipolar Disord. 2008; 10: 163–178.
Villringer A, Dirnagl U. Coupling of brain activity and cerebral blood flow: basis of functional neuroimaging. Cerebrovasc. Brain Metab. Rev. 1995; 7: 240–276.
Walther S, Hügli S, Höfle O, Federspiel A, Horn H, Bracht T, et al. Frontal white matter integrity is related to psychomotor retardation in major depression. Neurobiol. Dis. 2012; 47: 13–19.
Weinberger DR. Implications of Normal Brain Development for the Pathogenesis of Schizophrenia. Arch. Gen. Psychiatry 1987; 44: 660–669.
Wijeratne C, Sachdev S, Wen W, Piguet O, Lipnicki DM, Malhi GS, et al. Hippocampal and amygdala volumes in an older bipolar disorder sample. Int. Psychogeriatrics 2013; 25: 54–60.
Wilke M, Kowatch RA, DelBello MP, Mills NP, Holland SK. Voxel-based morphometry in adolescents with bipolar disorder: first results. Psychiatry Res 2004; 131: 57–69.
Womer FY, Wang L, Alpert KI, Smith MJ, Csernansky JG, Barch DM, et al. Basal ganglia and thalamic morphology in schizophrenia and bipolar disorder. Psychiatry Res. - Neuroimaging 2014; 223: 75–83.
Wood GE, Young LT, Reagan LP, Chen B, McEwen BS. Stress-induced structural remodeling in hippocampus: prevention by lithium treatment. Proc. Natl. Acad. Sci. U. S. A. 2004; 101: 3973–8.
Wylie GR, Genova H, DeLuca J, Chiaravalloti N, Sumowski JF. Functional magnetic resonance imaging movers and shakers: does subject-movement cause sampling bias? Hum. Brain Mapp. 2014; 35: 1–13.
Young RC, Biggs JT, Ziegler VE, Meyer DA. A rating scale for mania: Reliability, validity and sensitivity. Br. J. Psychiatry 1978; 133: 429–435.
Yucel K, McKinnon MC, Taylor VH, Macdonald K, Alda M, Young LT, et al. Bilateral hippocampal volume increases after long-term lithium treatment in patients with bipolar disorder: A longitudinal MRI study. Psychopharmacology (Berl). 2007; 195: 357–367.
Yucel K, Taylor VH, McKinnon MC, Macdonald K, Alda M, Young LT, et al. Bilateral hippocampal volume increase in patients with bipolar disorder and short-term lithium treatment. Neuropsychopharmacology 2008; 33: 361–7.
Zanetti M V., Jackowski MP, Versace A, Almeida JRC, Hassel S, Duran FLS, et al. State-dependent microstructural white matter changes in bipolar I

depression. Eur. Arch. Psychiatry Clin. Neurosci. 2009; 259: 316–328.
Zanetti M V., Otaduy MC, De Sousa RT, Gattaz WF, Busatto GF, Leite CC, et al. Bimodal effect of lithium plasma levels on hippocampal glutamate concentrations in bipolar II depression: A pilot study. Int. J. Neuropsychopharmacol. 2015; 18: 1–9.
Zhou Y, Yu C, Zheng H, Liu Y, Song M, Qin W, et al. Increased neural resources recruitment in the intrinsic organization in major depression. J. Affect. Disord. 2010; 121: 220–230.
Zhu X, Wang X, Xiao J, Liao J, Zhong M, Wang W, et al. Evidence of a dissociation pattern in resting-state default mode network connectivity in first-episode, treatment-naive major depression patients. Biol. Psychiatry 2012; 71: 611–617.

APPENDIX I

Voxel-based morphometry

Voxel-based morphometry (VBM) is an sMRI technique that measures brain tissue concentrations and makes inferences about the brain on the basis of differences in tissue classifications. Strictly speaking, it is a post-processing method of morphological images, however, I considered it here as it is used widely in neuropsychiatric research. Indeed, the technique has been reliably used in psychiatric research for many years (Job *et al.*, 2003; Spencer *et al.*, 2007), however it has not made a transition into the clinical arena. The VBM technique is heavily dependent on statistical and computational evaluation of differences in tissue classes. Indeed, it is a computationally and time intensive neuroimaging technique that can provide detailed information relating to changes in grey-white matter composition within the brain. The technique is based on a series of computational steps that correct the MR images for large-scale differences in gross anatomy prior to statistical evaluation. The computational steps include: (i) spatial normalization of all the images to a common reference space or template. The purpose of this step is to correct for global differences in brain shape; (ii) the segmentation of tissue classes into grey matter, white matter and cerebrospinal fluid. To assist the segmentation process,

the intensity of the structural images is often corrected for inhomogeneities caused by technical issues relating to the MRI head coil; and (iii) the final step involves smoothing the segmented grey and white matter images, which helps to compensate for the inexact nature of the normalization process. Large sample sizes are needed for identifiable changes to achieve statistical significance. Hence, currently it is not a technique that can be used to investigate changes in grey and white matter composition in individual patients. Another limitation of VBM is that it assumes the brain consists purely of grey matter, white matter and cerebrospinal fluid. This makes analysis of groups with pathologies such as tumor and stroke using normalization and segmentation procedures very difficult (Mechelli *et al.*, 2005).

Appendix II

Freesurfer segmentation

This procedure automatically segments and labels each anatomic structure based upon an atlas containing probabilistic information on the location of structures. This technique automatically assigns a neuroanatomical label to each voxel in a MRI volume based on probabilistic information estimated from a manually-labeled training set. The first stage is an affine registration with Talairach space followed by an initial volumetric labeling and correction from variation in intensity due to "intensity field bias." Finally, a high dimensional non-linear volumetric alignment to the Talairach atlas is performed and the volume is labeled. The labeling uses an algorithm based on both a subject-independent probabilistic atlas and subject-specific measured values assigning a value at each point in the space using three types of probabilities: 1) the probability of a given point to belong to each of the label classes; 2) the probability that a given point belongs to a label classes given its neighboring points; and 3) the probability distribution function (for volume-based labeling is measured by the intensity at that voxel) of the measured value is estimated separately for each class at each point (Fischl *et al.*, 2002, 2004). This method provides advantages similar

to manual region-of-interest (ROI) drawing (Jovicich *et al.*, 2009; Morey *et al.*, 2009), without the risk of biases, offering an anatomically accurate rendering of regional volumes (Fischl *et al.*, 2002).

APPENDIX III

Shape Analysis

Segmentations of seven bilateral subcortical grey matter nuclei (accumbens, amygdala, caudate, hippocampus, globus pallidus, putamen and thalamus) were generated using the FIRST algorithms included in the FMRIB Software Library (FSL, version 5.0.0). FIRST is a fully automated model-based segmentation/registration software, providing analyzing tools both for volume estimations and localized differences in shape (http://fsl.fmrib.ox.ac.uk/fsl/fslwiki/FIRST).

The segmentation process is based on the shape and appearance models, constructed from 336 manually segmented images using Gaussian assumptions combined with a Bayesian probabilistic approach (Patenaude et al., 2011). Specifically, FIRST algorithms ascertain the most probable shape by means of linear combinations of shape variations employing the learned manually segmented models. Moreover, the segmentation process includes boundary correction and registration to a MNI152 template using 12 degrees of freedom as well as a subcortical mask to detect and eliminate voxels outside the subcortical structure. Shape was then expressed as a mean with modes of variation (principal components) (ibidem).

After the automated segmentation by the software, the outputs need to be manually checked and confirmed for the proper nuclei extraction of all the subcortical structures.